

Abstract

Chemistry transport models determine the evolving chemical state of the atmosphere by solving the fundamental equations that govern physical and chemical transformations subject to initial conditions of the atmospheric state and surface boundary conditions, e.g., surface emissions. The development of data assimilation techniques synthesize model predictions with measurements in a rigorous mathematical framework that provides observational constraints on these conditions.

Two families of data assimilation methods are currently widely used: variational and Kalman filter (KF). The variational approach is based on control theory and formulates data assimilation as a minimization problem of a cost functional that measures the model-observations mismatch. The Kalman filter approach is rooted in statistical estimation theory and provides the analysis covariance together with the best state estimate. Suboptimal Kalman filters employ different approximations of the covariances in order to make the computations feasible with large models. Each family of methods has both merits and drawbacks.

This paper compares several data assimilation methods used for global chemical data assimilation. Specifically, we evaluate data assimilation approaches for improving estimates of the summertime global tropospheric ozone distribution in August 2006 based on ozone observations from the NASA Tropospheric Emission Spectrometer and the GEOS-Chem chemistry transport model. The resulting analyses are compared against independent ozonesonde measurements to assess the effectiveness of each assimilation method. All assimilation methods provide notable improvements over the free model simulations, which differ from the ozonesonde measurements by about 20 % (below 200 hPa). Four dimensional variational data assimilation with window lengths between five days and two weeks is the most accurate method, with mean differences between analysis profiles and ozonesonde measurements of 1–5 %. Two sequential assimilation approaches (three dimensional variational and suboptimal KF), although derived from different theoretical considerations, provide similar ozone estimates, with relative differences of 5–10 % between the analyses and ozonesonde measurements.

Comparison of chemical data assimilation schemes

K. Singh et al.

Title Page

Abstract

Introduction

Conclusions

References

Tables

Figures

⏪

⏩

◀

▶

Back

Close

Full Screen / Esc

Printer-friendly Version

Interactive Discussion



Adjoint sensitivity analysis techniques are used to explore the role of uncertainties in ozone precursors and their emissions on the distribution of tropospheric ozone. A novel technique is introduced that projects 3-D-Variational increments back to an equivalent initial condition, which facilitates comparison with 4-D variational techniques.

1 Introduction

Understanding the distribution of tropospheric ozone is one of the principal scientific challenges in global atmospheric chemistry, e.g., Jacob (1999). Ozone is an integral constituent of the troposphere that plays a significant role in determining the chemical and radiative state of the atmosphere. Ozone in the stratosphere absorbs UV radiation, which is harmful to human health. In the upper troposphere ozone is a greenhouse gas through absorption of upwelling long wave radiation. In the mid-troposphere ozone is a precursor to OH radicals which moderate pollution levels. At the surface ozone is a pollutant causing respiratory problems and affecting crop yields.

Numerous studies have attempted to quantify the distribution of tropospheric ozone through chemical transport models. The findings from these studies vary significantly due to the strong variability in ozone lifetimes and uncertainties in determining the amount of ozone lost through dry deposition, entered through upper troposphere-stratosphere exchanges, or evolved due to chemical reactions of trace gas and emission precursors. The ozone lifetime varies from a few minutes at the surface, to a few days in the lower troposphere, to months in the upper troposphere. In such situations, it is important to validate the accuracy of model predictions against observed state of the atmosphere. Studies of variations in tropospheric ozone have been conducted through ozonesonde measurements, surface measurements (Logan, 1994, 1999; Tarasick et al., 2005; Oltmans et al., 2006), and satellite observations (Munro et al., 1998; Tellmann et al., 2004).

Comparison of chemical data assimilation schemes

K. Singh et al.

Title Page

Abstract

Introduction

Conclusions

References

Tables

Figures

◀

▶

◀

▶

Back

Close

Full Screen / Esc

Printer-friendly Version

Interactive Discussion



**Comparison of
chemical data
assimilation schemes**K. Singh et al.

[Title Page](#)[Abstract](#)[Introduction](#)[Conclusions](#)[References](#)[Tables](#)[Figures](#)[◀](#)[▶](#)[◀](#)[▶](#)[Back](#)[Close](#)[Full Screen / Esc](#)[Printer-friendly Version](#)[Interactive Discussion](#)

Chemical data assimilation is a process of optimally combining imperfect observations with imperfect model simulations to produce a better estimate of the chemical state of the atmosphere and its boundary conditions (Carmichael et al., 2008). Considerable experience with data assimilation has been accumulated in the field of numerical weather prediction (Daley, 1991; Courtier et al., 1998; Rabier et al., 2000; Kalnay, 2002; Navon, 2009). In this work we focus on atmospheric constituent data assimilation. Chemical data assimilation poses specific challenges related to the multiphysics nature of the system, the stiffness of chemical kinetic equations, the sparseness of chemical observations, and the uncertainty in the levels of anthropogenic and natural pollutants emitted into the atmosphere. Throughout this paper we will refer to model results as model predictions or model forecasts even when a past period is simulated.

Previous studies have employed various approaches to assimilating observations of trace gases for improved tropospheric chemistry representations. Data assimilation has been used to improve initial conditions, boundary values (emissions), and has resulted in improved air quality forecasts. The base concepts of the variational approach to chemical data assimilation, and the construction of adjoint chemical transport models are discussed in detail in Sandu et al. (2005a); Hakami et al. (2007); Henze et al. (2007); Carmichael et al. (2008). Early work in chemical data assimilation using variational techniques has been reported in Khatatov et al. (2000); Elbern and Schmidt (2001). Since then there is a growing body of literature with applications of 3-D-Var and 4-D-Var chemical data assimilations. 3-D-Var was first used by Derber et al. (1991); Parrish and Derber (1992) and later applied by most of the meteorological centers (Courtier et al., 1998; Cohn et al., 1998; Gauthier et al., 1999a). A study on ozone improvement using 3-D-Var assimilation is presented in Bei et al. (2008). Adjustment of gas phase chemical tracer initial conditions has been studied in Chai et al. (2007); Sandu et al. (2005b); Tang et al. (2004); Zhang et al. (2008). Adjustment of pollutant emissions through 4-D-Var chemical data assimilation has been discussed in Chai et al. (2009). Data assimilation studies involving particle measurements to improve aerosol fields have been discussed in Hakami et al. (2005); Sandu et al. (2005b); Henze et al.

(2004, 2009). Suboptimal Kalman filters have been employed successfully for chemical data assimilation (Khattatov et al., 2000; Menard et al., 2000; Lamarque et al., 2002; Liao et al., 2006; Segers et al., 2005; Clark et al., 2006; Pierce et al., 2007; Parrington et al., 2009). The use of the ensemble Kalman filter (EnKF) (Evensen, 1994) in
5 chemical data assimilation has been studied in Constantinescu et al. (2007a,b,c).

Different approaches to data assimilation are rooted in different theories (control, statistical estimation), have different implementation and computational costs, and yield different performance on large scale problems of practical interest. A discussion on relationship between optimality of variational data assimilation and Kalman filters is presented in Li and Navon (2001). Houtekamer (2005) compared the quality of background statistics in 3-D-Var and EnKF using radiance observations from satellite, while, Laroche et al. (2005) compared the characteristics 3-D-Var and 4-D-Var introduced in the operational suite of the Canadian Meteorological Center (CMC). Constantinescu et al. (2007c) and Wu et al. (2008) compare the performances of EnKF with 4-D-Var
10 for chemical transport models on a regional scale using ground-level ozone measurements, while, Geer et al. (2006) provides an intercomparison of tropospheric ozone estimates obtained through 3-D-Var, 4-D-Var, and Kalman filter assimilation systems for both chemical transport and global circulation models as part of the Assimilation of ENVISAT Data (ASSET) project. The comparison between techniques in Wu et al. (2008) is done in the context of regional assimilation and using surface network data.

The Tropospheric Emission Spectrometer (TES) (Beer et al., 2001) is the first dedicated infrared instrument from which information of the global and vertical distribution of tropospheric ozone can be retrieved. Parrington et al. (2009) reported assimilation of vertical profiles of ozone from TES into the GEOS-Chem using suboptimal Kalman filter while Pierce et al. (2009) used TES and OMI in conjunction with a simple univariate filtering approach to investigate the impact of distant sources on air quality in Dallas and Houston. We have developed 3-D-Var and 4-D-Var data assimilation capabilities for GEOS-Chem v7. The goal of this paper is to provide the first direct comparison of global tropospheric ozone distribution estimated through 3-D-Var, 4-D-Var and
25

ACPD

11, 1–54, 2011

Comparison of chemical data assimilation schemes

K. Singh et al.

Title Page

Abstract

Introduction

Conclusions

References

Tables

Figures

◀

▶

◀

▶

Back

Close

Full Screen / Esc

Printer-friendly Version

Interactive Discussion



suboptimal KF assimilation systems showcasing the potential of TES profile retrievals. The assessment of analyses generated through different assimilation systems are on the similar lines of Geer et al. (2006); Parrington et al. (2009).

This paper is structured as follows: Sect. 2 provides the mathematical overview of how observations are integrated into the model in different data assimilation systems. Section 5.2 discusses the characteristics of background error covariance matrices used in this study. Section 3 provides a brief overview of the global chemical transport model (GEOS-Chem) and its adjoint development. A description of the TES instrument, its observation operator and profile retrieval formulation is provided in Sect. 4. Section 6 details the experimental settings, computational costs and assessment of tropospheric ozone estimates through different assimilation systems. Summary and points of future work are discussed in Sect. 7.

2 Chemical data assimilation

Variational methods solve the data assimilation problem in an optimal control framework (Sasaki, 1958; Le Dimet and Talagrand, 1986; Courtier and Talagrand, 1987; Lions, 1971). Specifically, they attempt to find the control variable values (e.g., initial conditions) by minimizing the discrepancy between the model forecast and observations subject to the governing dynamic equations. In contrast, statistical estimation methods (generically known as Kalman filters/smoothers) solve the data assimilation problem in a Bayesian framework by combining probability densities of errors from different sources (Khattatov et al., 2000; Menard et al., 2000; Lamarque et al., 2002; Segers et al., 2005; Clark et al., 2006; Pierce et al., 2007; Parrington et al., 2009; Constantinescu et al., 2007b,c). In the following discussion, for simplicity of presentation, we focus on discrete models (in time and space) where the initial conditions are the control variables.

Data assimilation provides best estimates of the state of the atmosphere by combining the following three sources of information.

Comparison of chemical data assimilation schemes

K. Singh et al.

Title Page

Abstract

Introduction

Conclusions

References

Tables

Figures

◀

▶

◀

▶

Back

Close

Full Screen / Esc

Printer-friendly Version

Interactive Discussion



Comparison of chemical data assimilation schemes

K. Singh et al.

Title Page

Abstract

Introduction

Conclusions

References

Tables

Figures

◀

▶

◀

▶

Back

Close

Full Screen / Esc

Printer-friendly Version

Interactive Discussion



1. The apriori, or background state \mathbf{x}^b represents the best estimate of the true state \mathbf{x}^t available before any measurements are taken. This estimate is assumed unbiased, and the random background (estimation) errors ε^b are typically assumed to have a normal probability density with a background error covariance matrix \mathbf{B}

$$\varepsilon^b = \mathbf{x}^b - \mathbf{x}^t \in \mathcal{N}(\mathbf{0}, \mathbf{B}). \quad (1)$$

2. The model encapsulates our knowledge about physical and chemical laws that govern the evolution of the system. The model evolves an initial state $\mathbf{x}_0 \in \mathbb{R}^n$ at the initial time t_0 to future state values $\mathbf{x}_i \in \mathbb{R}^n$ at future times t_i ,

$$\mathbf{x}_i = \mathcal{M}_{t_0 \rightarrow t_i}(\mathbf{x}_0). \quad (2)$$

The size of the state space in realistic chemical transport models is very large. For example, a GEOS-Chem simulation at the $2^\circ \times 2.5^\circ$ horizontal resolution has $n \in \mathcal{O}(10^8)$ variables.

3. Observations $\mathbf{x}_i^{\text{obs}} \in \mathbb{R}^m$ of the state are taken at times t_i , $1 = 1, \dots, N$

$$\mathbf{x}_i^{\text{obs}} = \mathcal{H}(\mathbf{x}_i) + \varepsilon_i^{\text{obs}}. \quad (3)$$

The observation operator \mathcal{H} maps the state space onto the observation space. In many practical situations \mathcal{H} is a highly nonlinear mapping, e.g., satellite radiance operators. The observations are characterized by measurement and representativeness errors $\varepsilon_i^{\text{obs}}$. The observation errors at each time are assumed to be independent of background errors, and independent of the observation errors at other times. They are typically assumed to have a normal distribution with mean zero and covariance \mathbf{R}_i ,

$$\varepsilon_i^{\text{obs}} \in \mathcal{N}(\mathbf{0}, \mathbf{R}_i). \quad (4)$$

Based on these three sources of information data assimilation computes the posterior estimate \mathbf{x}^a of the true state; \mathbf{x}^a is called the “analysis” state.

2.1 Three dimensional variational (3-D-Var) data assimilation

In the 3-D-Var data assimilation the observations (3) are considered successively at times t_1, \dots, t_N . The background state (i.e., the best state estimate at time t_i) is given by the model forecast, starting from the previous analysis (i.e., best estimate at time t_{i-1}):

$$\mathbf{x}_i^b = \mathcal{M}_{t_{i-1} \rightarrow t_i}(\mathbf{x}_{i-1}^a).$$

The discrepancy between the model state \mathbf{x}_i and observations at time t_i , together with the departure of the state from the model forecast \mathbf{x}_i^b , are measured by the 3-D-Var cost function:

$$\mathcal{J}(\mathbf{x}_i) = \frac{1}{2}(\mathbf{x}_i - \mathbf{x}_i^b)^T \mathbf{B}^{-1}(\mathbf{x}_i - \mathbf{x}_i^b) + \frac{1}{2}(\mathcal{H}(\mathbf{x}_i) - \mathbf{x}_i^{\text{obs}})^T \mathbf{R}_i^{-1}(\mathcal{H}(\mathbf{x}_i) - \mathbf{x}_i^{\text{obs}}) \quad (5)$$

While in principle a different background covariance matrix should be used at each time, in practice the same matrix is re-used throughout the assimilation window. The 3-D-Var analysis is computed as the state which minimizes (5)

$$\mathbf{x}_i^a = \text{argmin } \mathcal{J}(\mathbf{x}_i). \quad (6)$$

Typically a gradient-based numerical optimization procedure is employed to solve (6). The gradient $\nabla \mathcal{J}$ of the cost function (5) is

$$\nabla \mathcal{J}(\mathbf{x}_i) = \mathbf{B}^{-1}(\mathbf{x}_i - \mathbf{x}_i^b) + \mathbf{H}_i^T \mathbf{R}_i^{-1}(\mathcal{H}(\mathbf{x}_i) - \mathbf{x}_i^{\text{obs}}) \quad (7)$$

Note that the gradient requires to computation of the linearized observation operator $\mathbf{H}_i = \mathcal{H}'(\mathbf{x}_i)$ about the current state \mathbf{x}_i .

Preconditioning is often used to improve convergence of the numerical optimization problem (6). A change of variables is performed by shifting the state and scaling it with the square root of covariance:

$$\hat{\mathbf{x}}_i = \mathbf{B}^{1/2} (\mathbf{x}_i - \mathbf{x}_i^b), \quad (8)$$

and carrying out the optimization with the new variables $\hat{\mathbf{x}}_i$.

2.2 Four dimensional variational (4-D-Var) data assimilation

In strongly-constrained 4-D-Var data assimilation all observations (3) at all times t_1, \dots, t_N are simultaneously considered. The control parameters are the initial conditions \mathbf{x}_0 ; they uniquely determine the state of the system at all future times via the model Eq. (2).

The discrepancy between model predictions and observations at all future times t_1, \dots, t_N , together with the departure of the initial state from the background state, are measured by the 4-D-Var cost function:

$$\mathcal{J}(\mathbf{x}_0) = \frac{1}{2} (\mathbf{x}_0 - \mathbf{x}_0^b)^T \mathbf{B}^{-1} (\mathbf{x}_0 - \mathbf{x}_0^b) + \frac{1}{2} \sum_{i=1}^N (\mathcal{H}(\mathbf{x}_i) - \mathbf{x}_i^{\text{obs}})^T \mathbf{R}_i^{-1} (\mathcal{H}(\mathbf{x}_i) - \mathbf{x}_i^{\text{obs}}) \quad (9)$$

Note that the departure of the initial conditions from the background is weighted by the inverse background covariance matrix, \mathbf{B}^{-1} , while the differences between the model predictions $\mathcal{H}(\mathbf{x}_i)$ and observations $\mathbf{x}_i^{\text{obs}}$ are weighted by the inverse observation error covariances, \mathbf{R}_i^{-1} .

The 4-D-Var analysis is computed as the initial condition which minimizes (9) subject to the model equation constraints (2)

$$\mathbf{x}_0^a = \text{argmin } \mathcal{J}(\mathbf{x}_0) \quad \text{subject to (2)}. \quad (10)$$

The model (2) propagates the optimal initial condition (9) forward in time to provide the analysis at future times, $\mathbf{x}_i^a = \mathcal{M}_{t_0 \rightarrow t_i}(\mathbf{x}_0^a)$.

The optimization problem (10) is solved numerically using a gradient-based technique. The gradient of (9) reads

$$\nabla J(\mathbf{x}_0) = \mathbf{B}^{-1} \left(\mathbf{x}_0 - \mathbf{x}_0^b \right) + \sum_{i=1}^N \left(\frac{\partial \mathbf{x}_i}{\partial \mathbf{x}_0} \right)^T \mathbf{H}_i^T \mathbf{R}_i^{-1} \left(\mathcal{H}(\mathbf{x}_i) - \mathbf{x}_i^{\text{obs}} \right) \quad (11)$$

The 4-D-Var gradient requires not only the linearized observation operator \mathbf{H}_i , but also the transposed derivative of future states with respect to the initial conditions. The 4-D-Var gradient can be obtained effectively by forcing the adjoint model with observation increments, and running it backwards in time.

5 2.3 Suboptimal Kalman filter

The suboptimal Kalman filter is a sequential data assimilation approach (Khattatov et al., 2000) in which corrections in the concentration state vector are performed as soon as observations become available. Similar to 3-D-Var, for every observation time t_i , this technique starts with the model forecast state (\mathbf{x}_i^f) and provides an expected analysis state (\mathbf{x}_i^a) that reduces the discrepancy between the model forecast and the observations $\mathbf{x}_i^{\text{obs}}$. The analysis state vector is obtained as

$$\mathbf{x}_i^a = \mathbf{x}_i^f + \mathbf{K}_i \left(\mathbf{x}_i^{\text{obs}} - \mathcal{H}(\mathbf{x}_i^f) \right) \quad (12)$$

where \mathbf{K} is the Kalman gain matrix, \mathbf{H} is the observation operator defined in Eq. (3), and \mathbf{x}^{obs} the vector of observations at a given time. The Kalman gain matrix is defined as

$$\mathbf{K}_i = \mathbf{P}_i^f \mathbf{H}^T \left(\mathbf{H}_i \mathbf{P}_i^f \mathbf{H}_i^T + \mathbf{R}_i \right)^{-1} \quad (13)$$

where \mathbf{P}_i^f is the forecast error covariance matrix, \mathbf{R}_i is the observation error covariance matrix (4), and $\mathbf{H}_i = \mathcal{H}'(\mathbf{x}_i^f)$ is the linearized observation operator about the forecast

Comparison of chemical data assimilation schemes

K. Singh et al.

Title Page

Abstract

Introduction

Conclusions

References

Tables

Figures

◀

▶

◀

▶

Back

Close

Full Screen / Esc

Printer-friendly Version

Interactive Discussion



state. If a diagonal or block-diagonal approximation of the error covariance matrix \mathbf{P}^f is used in Eq. (13), the analysis state generated through Eq. (12) is suboptimal. A description on the structure of \mathbf{P}^f is provided in Sect. 5.2.

At each observation time, along with the analysis state, the analysis error covariance matrix \mathbf{P}_i^a is also calculated as

$$\mathbf{P}_i^a = (\mathbf{I} - \mathbf{K}_i \mathbf{H}_i) \mathbf{P}_i^f \quad (14)$$

where \mathbf{I} is the identity matrix. There are multiple ways in which this analysis covariance matrix is made available to the next observation window. A simple approach is to keep the analysis covariance equal to the background covariance for the entire assimilation period (Parrington et al., 2009). Here we build diagonal approximations to \mathbf{P}_{i+1}^f by transporting variances (diagonal entries in \mathbf{P}_i^a) as passive tracers following Menard et al. (2000).

3 GEOS-Chem

In this paper we specifically consider GEOS-Chem (<http://geos-chem.org>), a global three-dimensional chemical transport model (CTM) driven by assimilated meteorological fields from Goddard Earth Observing System (GEOS-4) at the NASA Global Modeling and Assimilation Office (GMAO). It is being widely used by research groups world-wide for performing global atmospheric chemistry studies. The model along with comparison of model predictions with observations was first described in Bey et al. (2001). GEOS-Chem accounts in detail for emissions from both natural and anthropogenic sources, for gas phase chemistry, aerosol processes, long range transport of pollutants, troposphere-stratosphere exchanges, etc. Anthropogenic emissions are obtained from the Global Emissions Inventory Activity (GEIA) (Benkovitz et al., 1996) while lightning NO_x source emissions are estimated using Price and Rind (1992), based on deep convective cloud top heights provided with the GMAO meteorological fields. Biomass burning emissions are based on Duncan et al. (2003) while biofuel

Comparison of chemical data assimilation schemes

K. Singh et al.

Title Page

Abstract

Introduction

Conclusions

References

Tables

Figures

◀

▶

◀

▶

Back

Close

Full Screen / Esc

Printer-friendly Version

Interactive Discussion



emissions are from Yevich and Logan (2003). The meteorological fields have a horizontal resolution of 1° along latitude and 1.25° along longitude with 55 vertical levels, and a temporal resolution of 6 h (3 h for surface fields). We use GEOS-Chem v7.2.3. Subsequent model releases and references can be found at <http://geos-chem.org>.

The GEOS-Chem Adjoint system (http://wiki.seas.harvard.edu/geos-chem/index.php/GEOS-Chem_Adjoint) has been developed through a joint effort of groups at Virginia Tech, University of Colorado, Caltech, Jet Propulsion Laboratory, and Harvard (Henze et al., 2007; Singh et al., 2009a,b; Eller et al., 2009). The system can perform adjoint sensitivity analyses and 4-D-Var chemical data assimilation. Inverse modeling studies with GEOS-Chem-Adjoint are exemplified in Henze et al. (2009); Kopacz et al. (2007); Zhang et al. (2009).

4 Tropospheric Emission Spectrometer (TES) observations

TES (Beer et al., 2001), one of four science instruments aboard NASA's Aura satellite, measures top-of-the-atmosphere high resolution spectrally-resolved longwave radiation (<http://tes.jpl.nasa.gov>). Vertical profiles of chemical concentrations are inferred from these radiance measurements using an off-line inversion process (Bowman et al., 2006). In this work we assimilate the retrieved ozone vertical profiles. Figure 1 shows the location of TES profiles for two days. Only TES profiles between 60° S– 60° N are considered because of the lower poleward thermal contrast.

A-priori information about the vertical concentration profile of the species of interest is needed to solve the retrieval inverse problem (the prior information does not come from the measurement). Let $\mathbf{x}^{\text{prior}}$ be the prior vertical ozone concentration profile (in volume mixing ratio units), and let $\mathbf{z}^{\text{prior}} = \log \mathbf{x}^{\text{prior}}$. Let $\mathbf{z}^{\text{true}} (= \log \mathbf{x}^{\text{true}})$ be the “true” atmospheric profile.

Comparison of chemical data assimilation schemes

K. Singh et al.

Title Page

Abstract

Introduction

Conclusions

References

Tables

Figures

◀

▶

◀

▶

Back

Close

Full Screen / Esc

Printer-friendly Version

Interactive Discussion



The vertical ozone profile retrieval can be expressed according to the formula

$$\hat{\mathbf{z}} = \mathbf{z}^{\text{prior}} + \mathbf{A} \left(\mathbf{z}^{\text{true}} - \mathbf{z}^{\text{prior}} \right) + \mathbf{G}\eta, \quad \hat{\mathbf{x}} = \exp(\hat{\mathbf{z}}). \quad (15)$$

Here \mathbf{A} is the averaging kernel matrix, \mathbf{G} is the gain matrix, and η is the spectral measurement error (assumed to have mean zero and covariance \mathbf{S}_η). More details can be found in Bowman et al. (2002); Jones et al. (2003); Worden et al. (2004).

The corresponding TES observation operator \mathcal{H} is linear with respect to the logarithm of the concentrations, but nonlinear with respect to the concentration profile:

$$\mathcal{H}(\mathbf{x}) = \mathbf{z}^{\text{prior}} + \mathbf{A} \left(\log(\mathbf{L}\mathbf{x}) - \mathbf{z}^{\text{prior}} \right) \quad (16)$$

where \mathbf{L} is an interpolation operator that transforms \mathbf{x} from the GEOS-Chem N -level vertical grid to the TES profile retrieval P -level grid.

For this reason several chemical data assimilation studies based on TES retrieved profiles (Jones et al., 2003; Bowman et al., 2006; Parrington et al., 2009) have opted to perform the suboptimal Kalman filtering step (12) in the logarithm of the concentrations:

$$\log \mathbf{x}^a = \log \mathbf{x}^f + \mathbf{K} \left(\hat{\mathbf{z}} - \mathcal{H}(\mathbf{x}^f) \right)$$

Here \mathbf{K} is the Kalman gain matrix, \mathcal{H} is the observation operator defined in Eq. (16), and $\hat{\mathbf{z}}$ is the ozone profile retrievals from TES as described in Eq. (15). The analysis state is calculated in natural logarithm of volume mixing ratio (log VMR) at each observation grid point since the TES profile retrievals are in log VMR. An exponential operator and a linear interpolation operator based on pressure is then applied to this logarithm of analysis state in succession to regain the actual analysis state in GEOS-Chem grid domain. The points which do not lie on the observation grid remain unaffected by the assimilation.

The observation operator \mathcal{H} that transforms higher resolution model state to the TES profile vertical grid (observation grid) domain is expressed by Eq. (16). The Kalman

Comparison of chemical data assimilation schemes

K. Singh et al.

Title Page

Abstract

Introduction

Conclusions

References

Tables

Figures

◀

▶

◀

▶

Back

Close

Full Screen / Esc

Printer-friendly Version

Interactive Discussion



gain matrix \mathbf{K} is defined by Eq. (13), particularized to the case where the state is the logarithm of volume mixing ratio.

For variational data assimilation the forcing calculation is carried out in concentrations. For this reason, an adjoint of the observation operator needs to be derived to update the gradients as described in Eqs. (7) and (11)

$$\mathbf{H}^T \cdot \mathbf{v} = \left(\frac{\partial}{\partial \mathbf{x}} (\mathbf{A} \log(\mathbf{Lx})) \right)^T \cdot \mathbf{v} = \mathbf{L}^T \cdot \begin{pmatrix} (\mathbf{Lx})_0^{-1} & 0 & \dots & 0 \\ 0 & (\mathbf{Lx})_1^{-1} & \dots & 0 \\ \vdots & \vdots & \ddots & \vdots \\ 0 & 0 & \dots & (\mathbf{Lx})_P^{-1} \end{pmatrix} \cdot \mathbf{A}^T \cdot \mathbf{v}$$

Here, $\mathbf{H} = \mathcal{H}'(\mathbf{x})$ is a matrix and $\mathbf{v} = \mathbf{R}^{-1} (\mathcal{H}(\mathbf{x}) - \mathbf{x}^{\text{obs}})$. The TES averaging kernel \mathbf{A} is usually a non-symmetric matrix, and the result of $\mathbf{A}^T \cdot \mathbf{v}$ is fed to the interpolation operator to construct the diagonal matrix with the i -th element being $1/(\mathbf{Lx})_i$. The term \mathbf{L}^T is the adjoint of the interpolation operator and brings entities from the TES profile retrieval domain back to the GEOS-Chem model domain.

Note that the TES data can be biased by as much as 10 % (Nassar et al., 2008). We have estimated the bias using the technique proposed in Nassar et al. (2008) and have removed it before assimilating the data.

5 Experimental setting for data assimilation

For numerical experiments, we employ GEOS-Chem v7-04-10 adjoint code package (Singh et al., 2009b), capable of performing both 3-D-Var and 4-D-Var data assimilations with real data. It also incorporates suboptimal Kalman filter approach of data assimilation developed in Parrington et al. (2009). We assimilate Tropospheric Emission Spectrometer (TES) satellite ozone profile retrievals into the GEOS-Chem model and validate the generated analyses against an independent observation dataset provided

Comparison of chemical data assimilation schemes

K. Singh et al.

Title Page

Abstract

Introduction

Conclusions

References

Tables

Figures

◀

▶

◀

▶

Back

Close

Full Screen / Esc

Printer-friendly Version

Interactive Discussion



by direct ozone profile measurements from ozonesondes. The numerical optimization method used in all variational experiments is the limited memory bound-constrained BFGS (Zhu et al., 1997). This quasi-Newton approach has become the “gold standard” in solving large scale chemical data assimilation problems (Sandu et al., 2005a).

5 Simulations with GEOS-Chem v7 adjoint can be carried out at $4^\circ \times 5^\circ$ and $2^\circ \times 2.5^\circ$ resolutions. We have used $4^\circ \times 5^\circ$ resolution in all our experiments. There are 46×72 latitude-longitude grid boxes at this resolution, and 55 vertical levels; near the equator and at ground level each grid box covers an area of about $400 \text{ km} \times 500 \text{ km}$. The model has been modified to use the linearized ozone (linoz) scheme (McLinden et al., 2000) for a better estimation of ozone exchanges at troposphere-stratosphere boundary. This scheme is available in v8 and above (see <http://geos-chem.org>). We performed data assimilation for only the first 23 model levels (for up to about 50 hPa), which encompasses where TES observations are most sensitive.

5.1 Data assimilation schemes

15 The 3-D-Var data assimilation experiments were performed for a period of two weeks in the month of August 2006, starting at 00:00 (GMT) on August 1st. The TES data was read once every four simulation hours; the observation operator called at model time t (hours) reads in all the measurements collected within the interval $t - 2$ (hours) to $t + 2$ (hours). 3-D-Var data assimilation treats all observations in this interval as instantaneous, and assimilates them in the same optimization run. In all our 3-D-Var experiments, we performed 8 iterations per analysis since the cost function decreased significantly within the first few iterations. It is important to note that 3-D-Var does not involve any model adjoint calculations; gradients require only the adjoint of the observation operator. The optimization adjusts ozone concentrations. The generated analysis profile at the end of each observation window is evolved through the forward model that becomes the initial condition for the next observation window. It is also important to mention here that a new background error covariance matrix (17) is constructed for every observation window.

Comparison of chemical data assimilation schemes

K. Singh et al.

Title Page

Abstract

Introduction

Conclusions

References

Tables

Figures

◀

▶

◀

▶

Back

Close

Full Screen / Esc

Printer-friendly Version

Interactive Discussion



Comparison of chemical data assimilation schemes

K. Singh et al.

Title Page

Abstract

Introduction

Conclusions

References

Tables

Figures

⏪

⏩

◀

▶

Back

Close

Full Screen / Esc

Printer-friendly Version

Interactive Discussion



The setup for data assimilation using the suboptimal Kalman filter is quite similar to 3-D-Var where we assimilated TES profile retrievals into GEOS-Chem over a two week period from 00:00 GMT on 1 August 2006 to 00:00 GMT on 15 August 2006. Observations were read every 4 hours and analysis states were generated for each observation window through the sequential update formula (12).

The 4-D-Var data assimilation experiments were performed for two different assimilation window lengths to adjudge if model errors hamper the quality of assimilations in GEOS-Chem involving longer assimilation windows; 4-D-Var is strongly constrained by the forward model Eq. (10). Starting at 00:00 GMT on 1 August 2006, the first assimilation window is considered to be of five days while the second window is of two weeks. All the three assimilation systems had the same initial conditions to start with and were generated through a free GEOS-Chem model run. There were 12 optimization iterations performed in order to improve the ozone initial condition. Each iteration during 4-D-Var assimilation includes a forward model and a backward model adjoint run. TES profile retrievals were read every 4 h during the model adjoint run, and the cost function and adjoint gradients accumulated the impact of all 4 h data sets throughout the assimilation window. Contrary to 3-D-Var and suboptimal KF, where analysis states are generated sequentially every observation window, in 4-D-Var the analysis is generated only at the initial time and accounts for the mismatch between observations and model predictions over all the observations in the assimilation window.

5.2 Specification of error variances

We consider a diagonal background error covariance matrix (\mathbf{B}) in all our variational data assimilation experiments for simplicity. The initial variances (the diagonal entries of the \mathbf{B} matrix) are constructed from the average background concentrations \mathbf{x}_0^B on each of the Nlev model vertical layers

$$\mathbf{B} = \begin{bmatrix} \mathbf{B}^{(0)} & 0 \dots & 0 \\ 0 & \mathbf{B}^{(1)} & \dots & 0 \\ \vdots & \ddots & & \vdots \\ 0 & 0 \dots & \mathbf{B}^{(Nlev)} \end{bmatrix} \quad (17)$$

where

$$\mathbf{B}^{(\ell)} = \begin{bmatrix} \sigma_\ell^2 & 0 \dots & 0 \\ 0 & \sigma_\ell^2 \dots & 0 \\ \vdots & \ddots & \vdots \\ 0 & 0 \dots & \sigma_\ell^2 \end{bmatrix}_{\text{dim} \times \text{dim}}, \quad \text{dim} = Nlon \cdot Nlat, \quad (18)$$

with

$$\sigma_\ell = \frac{\alpha_{rel}}{\text{dim}} \sum_{i=1}^{Nlon} \sum_{j=1}^{Nlat} \mathbf{x}_0^B(i, j, \ell, s_{O_3}), \quad \ell = 1, \dots, Nlev, \quad s_{O_3} = \text{index of ozone}. \quad (19)$$

The relative uncertainty level in the background initial conditions (i.e., at the beginning of the assimilation window) is taken to be 50 %, i.e., $\alpha_{rel} = 0.5$.

The forecast error covariance matrix \mathbf{P}_0^f used in our suboptimal Kalman filter approach is diagonal. The initial forecast error is assumed to be 50 % of the initial forecast field that is supposed to capture the representativeness error as well. In matrix form, \mathbf{P}_0^f is represented as

$$\mathbf{P}_0^f = \begin{bmatrix} \mathbf{P}_0^{f(0)} & 0 \dots & 0 \\ 0 & \mathbf{P}_0^{f(1)} & \dots & 0 \\ \vdots & \ddots & & \vdots \\ 0 & 0 \dots & \mathbf{P}_0^{f(Nobs)} \end{bmatrix} \quad (20)$$

where Nobs is the number of observation points (in our case, the number of grid points in the TES retrieval domain). The initial forecast error covariance matrix block corresponding to each observation grid point is given as

$$\mathbf{P}_0^{f(i)} = \alpha_{\text{rel}} \cdot \begin{bmatrix} \mathbf{x}_0^f(i, 1, s_{\text{O}_3}) & 0 & \dots & 0 \\ 0 & \mathbf{x}_0^f(i, 2, s_{\text{O}_3}) & \dots & 0 \\ \vdots & \ddots & \ddots & \vdots \\ 0 & 0 & \dots & \mathbf{x}_0^f(i, \text{Nret}, s_{\text{O}_3}) \end{bmatrix}_{\text{Nret} \times \text{Nret}}, \quad i = 1, 2, \dots, \text{Nobs}, \quad (21)$$

where Nret is the number of vertical TES profile retrieval levels. Although the initial forecast error covariance matrix \mathbf{P}^f and all analysis \mathbf{P}^a s henceforth are diagonal and there are no horizontal correlations being accounted for, the averaging kernels in the observation operator of TES as defined in Eq. (16) provide vertical correlations when operated on \mathbf{P}^f through Eq. (13). A detailed discussion on how to efficiently extend the background error covariance matrices to non-diagonal forms that capture spatial error correlations is provided in Singh et al. (2011a).

6 Data assimilation results

6.1 Computational costs

The 3-D-Var and suboptimal KF frameworks are built on top of GEOS-Chem v7 package which uses Sparse Matrix Vectorized GEAR (SMVGEAR) solver for chemistry. However, to construct the adjoint of chemistry required by the 4-D-Var, we implemented the Kinetic PreProcessor (KPP) solver (Damian et al., 2002) into GEOS-Chem which not only provides a suite of high performance chemical solvers to choose from but also generates automatically the continuous and discrete adjoint codes (Daescu, 2000, 2003; Sandu et al., 2003a,b). A detailed discussion on interfacing KPP with GEOS-Chem and comparison with native SMVGEAR solver for accuracy and computational

Title Page

Abstract

Introduction

Conclusions

References

Tables

Figures

◀

▶

◀

▶

Back

Close

Full Screen / Esc

Printer-friendly Version

Interactive Discussion



performance is presented in Eller et al. (2009). As pointed out in Henze et al. (2007), the computational cost of Rosenbrock solver increases significantly with the tolerance levels; higher tolerances use smaller internal time steps requiring more computation. In our experiments, we have set $RTOL = 10^{-3}$ and $ATOL = 10^{-2}$ to achieve moderate to high accuracy.

The suboptimal Kalman filter is less expensive than 3-D-Var since it generates the analysis through the single update formula (12), while 3-D-Var requires a few iterations before the optimization routine could generate a stable optimal analysis field. This is true however as long as the forecast error covariance matrix is diagonal. Once we move to non-diagonal matrices, the cost of calculating Kalman gain matrix (13) can be high, although this can be parameterized following, for example, Khattatov et al. (2000). In the case of 3-D-Var and 4-D-Var, using even full \mathbf{B} matrix adds a minimal cost to the overall simulation since the complete matrix is never constructed; at each step only a matrix vector product is required and efficient techniques are employed to derive the inverse and other powers of \mathbf{B} matrix (Singh et al., 2011a). The 4-D-Var assimilation is the most expensive of all the assimilation systems under consideration. The reason is attributed to the fact that a single 4-D-Var iteration performs both the forward and adjoint model runs, where, several variables on which the adjoint equation depends on, are written in checkpoint files in the forward model run.

Table 1 provides a comparison of the computational costs of the different data assimilation systems and the cost of free running model for a 24 h simulation. All the simulations are performed on a Dell Precision T5400 workstation with two quad-core Intel(R) Xeon(R) processors, with clock speed 2.33 GHz, and 16 GB of RAM shared between the two processors.

6.2 Comparison with ozonesonde measurements

In order to assess the quality of analysis fields generated through different assimilation systems, we use ozonesonde profiles measured by the INTEX Ozonesonde Network Study 2006 (IONS-6) (<http://croc.gsfc.nasa.gov/intexb/ions06.html> Thompson et

Comparison of chemical data assimilation schemes

K. Singh et al.

Title Page

Abstract

Introduction

Conclusions

References

Tables

Figures

⏪

⏩

◀

▶

Back

Close

Full Screen / Esc

Printer-friendly Version

Interactive Discussion



al., 2007a) for the month of August, assuming that these measurements provide values close to the true state of the atmosphere. There are 418 ozonesondes launched from 22 stations across North America as shown in the Fig. 1. A detailed description of the number of ozonesondes launched per station with longitude and latitude information can be found in Parrington et al. (2008). The ozonesonde observations are not used in data assimilation, and therefore provide an independent data set against which the analysis results are validated. Forecast scoring techniques using assimilated data as described in Wu et al. (2008); Constantinescu et al. (2007c) do not provide a fair assessment of the quality of assimilation for sparse spatio-temporal sampling and longer time scales used in this analysis.

We first consider the case where the assimilation window length is five days. As per the property of sequential data assimilation algorithms, the model forecast is corrected as soon as an observation is available. Ingesting observations every four simulation hours, we obtain an analysis field every four hours that accounts for the mismatch between the model prediction and the observations within that observation window. However, it is important to note that the model prediction at any observation window incorporates implicitly the corrections from all previous observations. Thus, as we move forward in time, the analysis field agrees better with the true state of the atmosphere. 4-D-Var on the other hand accumulates the forcing due to mismatch between model forecast and observations throughout the assimilation window to produce an initial condition that, when evolved forward in time through the model, will best fit the observations. Therefore, in the case of sequential assimilation approaches, to obtain a stable analysis state that resembles the true chemical state of the atmosphere at a particular instant, we need to start the simulation days or months prior to that instant to benefit from earlier observations. 4-D-Var is advantageous in situations where past observations are not available, as it provides the best estimate using only the observations available in the assimilation window under consideration.

We present in Fig. 2, a comparison of analysis profiles obtained from different assimilation systems, and free GEOS-Chem model run against ozonesonde measurement

Comparison of chemical data assimilation schemes

K. Singh et al.

[Title Page](#)[Abstract](#)[Introduction](#)[Conclusions](#)[References](#)[Tables](#)[Figures](#)[Back](#)[Close](#)[Full Screen / Esc](#)[Printer-friendly Version](#)[Interactive Discussion](#)

data. The left panel shows vertical ozone profiles (concentrations against pressure levels); the model predictions are sampled at the locations and times of ozonesonde measurements available in the 5-day assimilation window. The differences between model results and ozonesonde data reflect model prediction errors; one error vertical profile is obtained for each ozonesonde launch. The center and right panels show the mean and the standard deviation of these errors. The plots provide an assessment of the quality of tropospheric ozone estimates given by the free model run, and by data assimilation systems based on suboptimal Kalman filter, 3-D-Var and 4-D-Var approaches. The errors also reflect the impact of TES profile retrievals on these assimilation systems.

It is evident from the plots in Fig. 2 that 4-D-Var provided the best estimate for lower and mid troposphere ozone concentrations. The relative difference between the mean ozone analysis field and the ozonesonde measurements were decreased to less than 4% up to 180 hPa as compared to 5–20% in cases of suboptimal KF and 3-D-Var. The overestimate of ozone in the upper troposphere is likely due to the accumulated impact of the TES bias. The bias correction approach described in (Nassar et al., 2008) may not be sufficient for assimilation studies and suggests an on-line bias correction scheme may be needed in the future. There was also a substantial improvement in the variance of the assimilation relative to the ozonesonde measurements, particularly for the 4-D-Var case at 200 hPa. Consequently, the satellite observations have an impact not only on the mean value of tropospheric ozone but are also providing some additional information on the ozone distribution. A detailed analysis on the information brought in by TES profile retrievals into the 4-D-Var assimilation system at different pressure levels is provided in (Singh et al., 2011b).

Figure 3 provides the global tropospheric ozone distribution as estimated by GEOS-Chem free model run and different assimilation systems at the end of the 5 days run. The ozone concentration values are averaged over 10 GEOS-Chem levels (from the surface to about 370 hPa) for each longitude-latitude grid point on the horizontal domain.

Comparison of chemical data assimilation schemes

K. Singh et al.

[Title Page](#)[Abstract](#)[Introduction](#)[Conclusions](#)[References](#)[Tables](#)[Figures](#)[◀](#)[▶](#)[◀](#)[▶](#)[Back](#)[Close](#)[Full Screen / Esc](#)[Printer-friendly Version](#)[Interactive Discussion](#)

As seen in Fig. 3, all the assimilation systems seem to have caused an increase in the tropospheric ozone as compared to the model forecast with 4-D-Var bringing the highest amount. The gain seems to be prominent in the 30° N to 60° N latitude region in case of suboptimal KF and 3-D-Var, while it is extended up to 90° N in case of 4-D-Var. For a clear demonstration of these changes, we provide in Fig. 4, the plots of differences in the tropospheric ozone estimates through free model run and different assimilation systems.

In Fig. 4, panels a and b show that the structure of corrections in the ozone concentrations through 3-D-Var and suboptimal KF data assimilation are quite similar. The reason behind such a structure is that these sequential algorithms bring in instantaneous corrections based solely on the mismatch between the model predictions and the observations in an observation window (analysis cycle). The localized corrections here are mostly along the Aura satellite orbit. Panel c on the other hand showcases the smoother correction profile of 4-D-Var. In each 4-D-Var optimization iteration, the cost function and gradients are accumulated for all the observation windows where the adjoint variable (gradient) is flown backwards in time as governed by the model adjoint equation. The corrections brought in by the optimization routine therefore are no longer localized resulting in an ozone distribution consistent with the model dynamics and chemistry. We also plot the difference in the analysis fields obtained by 3-D-Var and suboptimal KF showcasing their close resemblance (panel d). Interestingly, there seems to be a localized overcorrection in the mid west Australian region by the sub-optimal Kalman filter. This overcorrection is likely due to the propagation of emissivity errors over the Australian desert in the TES retrieval, which can have possess strong silicate spectral signatures into the TES ozone retrieval. In this case, the 4-D-Var solution can smooth out localized satellite artifacts through the strong model constraint.

We next consider simulations with assimilation window length of 2 weeks. A longer assimilation window provides an insight into how ozone estimates due to assimilation evolve with time and if the corrections maintain structures similar to 5-day case. In particular, the ozone lifetime will limit the utility of ozone initial condition adjustment as the

Comparison of chemical data assimilation schemes

K. Singh et al.

Title Page

Abstract

Introduction

Conclusions

References

Tables

Figures

⏪

⏩

◀

▶

Back

Close

Full Screen / Esc

Printer-friendly Version

Interactive Discussion



assimilation window increases. It also helps adjudge if model errors in GEOS-Chem cause any degradation in the assimilation systems, especially the strongly constrained 4-D-Var.

Similar to Fig. 2, we present in Fig. 5, a comparison of analysis profiles obtained from different assimilation systems against ozonesonde measurement data. The plots reflect that the accuracy of suboptimal Kalman filter and 3-D-Var assimilations start to differ with longer assimilation window. While suboptimal KF underestimates ozone concentrations in the lower and mid troposphere, it performs better than 3-D-Var in the mid and upper tropospheric region. 4-D-Var still provided the best ozone estimate of all the assimilation systems, and, unlike the 5 days assimilation window length case, it performed well in the upper tropospheric region as well except near the tropopause. Panel c suggests that the standard deviation of 4-D-Var analysis from the ozonesonde measurements stayed the least among all the assimilation systems. The relative difference between the mean ozone analysis field and the ozonesonde measurements were decreased to less than 4 % up to 150 hPa as compared to 4–16 % in cases of suboptimal KF and 3-D-Var. With longer assimilation window, all the assimilation systems seem to have benefited from more observations being assimilated.

Figure 6 provides the global tropospheric ozone distribution as estimated by GEOS-Chem free model run and different assimilation systems. Similar to the 5 days assimilation window case, 4-D-Var leads to the maximum increase in the tropospheric ozone.

Figure 7 showcases the structure of corrections in model predicted ozone through different assimilation systems. The ozone corrections are up to 20 ppbv, and are consistent among the three assimilation schemes. The localized correction structure in 3-D-Var and suboptimal KF cases still persists with longer assimilation window. 4-D-Var provides larger corrections with a significant increase in ozone concentrations in the 30° N to 90° N latitude region. The reason for this difference can be explained in part by the restriction of the TES to 60° S–60° N, which limits where the corrections can be made in the 3-D-Var. Changes poleward of 60° N in the 3-D-Var solution are due to

Comparison of chemical data assimilation schemes

K. Singh et al.

Title Page

Abstract

Introduction

Conclusions

References

Tables

Figures

⏪

⏩

◀

▶

Back

Close

Full Screen / Esc

Printer-friendly Version

Interactive Discussion



forward advection. However, as discussed in Sect. 6.3.2, the elevated ozone poleward of 60° N in the 4-D-Var solution is due to the positive correction of high latitude initial conditions at the beginning of the assimilation window at 1 August 2006. Interestingly, the localized correction in the mid west Australian region which was not visible in the 3-D-Var case for 5 days assimilation window case, seems to be prominent in longer assimilation, while, in the case of suboptimal KF, it has been accentuated.

Contrary to what was observed in Wu et al. (2008) for the 4-D-Var assimilation in Polair3-D case where the accuracy of the ozone estimates decreased with increase in the assimilation window length, our findings show that the performance of the 4-D-Var system improves with increase of the assimilation window. However, this is likely due to the fact that the ozone lifetime is reasonably close to two weeks. Assimilation windows longer than two weeks would lead to a reduction in performance of the 4-D-Var system as the initial conditions become less important towards the end of the window. Consequently, the assimilation window for ozone in a 4-D-Var system should be bounded by the ozone lifetime. There is however one case where the accuracy of ozone estimates decrease with increase in assimilation window length for 4-D-Var and that is when the model adjoints are inaccurate. We have studied this case in detail in (Singh et al., 2011c) and have utilized inaccurate gradients to work towards our benefit in terms of reducing significantly the memory and computational costs, still maintaining the quality of the analysis.

6.3 Comparison of 3-D-Var and 4-D-Var

As discussed in Sect. 2, the 3-D-Var approach processes observations sequentially, and generates a new analysis every time new observations are available. The 3-D-Var corrections perform successive adjustments of the forward model trajectory, which decrease the error as more observations are being considered. The 4-D-Var approach, on the other hand, processes all observations at once and adjusts the initial conditions for the current assimilation window.

Comparison of chemical data assimilation schemes

K. Singh et al.

Title Page

Abstract

Introduction

Conclusions

References

Tables

Figures

◀

▶

◀

▶

Back

Close

Full Screen / Esc

Printer-friendly Version

Interactive Discussion



We compare the 3-D-Var and 4-D-Var approaches in two different ways. Section 6.3.1 discusses the ability of 4-D-Var to explicitly represent relationships between different chemical components. Section 6.3.2 proposes a variational approach to directly compare the use of information by the two methods.

6.3.1 Dependencies between multiple species

The data assimilation scenario discussed here corrects the ozone distribution in response to new information provided by ozone measurements. The new information is distributed implicitly to other state variables (e.g., other chemical species) through the model evolution (a change in ozone concentrations will result in different concentrations of other species after some time).

Can one explicitly represent, and apply, the corrections to other species resulting from ozone measurements? In order to perform explicit corrections of other chemical species, 3-D-Var requires an inter-species error correlation matrix. A correct specification of the inter-species correlation matrix at each observation time is a difficult task.

The 4-D-Var approach captures the causal relationship between species through the model dynamics (this holds even when the background covariance matrix does not specify inter-chemical correlations). In principle, it is possible to directly extend the set of control variables to include the initial conditions of all chemical species present in the model, together with the emission and deposition rates, and any other model parameters. The additional computational cost is minimal since the adjoint model already computes the derivatives with respect to all state variables (all concentrations), and any other sensitivity can be obtained by post-processing the adjoint fields. (Of course, extending the control vector may lead to separate issues related to convergence, and to the proper regularization of the problem).

The adjoint sensitivity analysis is by itself an important tool to investigate various dependencies between model parameters. The gradient formula (11) can be immediately extended to include derivatives of the cost function with respect to the initial conditions of other species besides ozone, and with respect to model parameters such as

Comparison of chemical data assimilation schemes

K. Singh et al.

Title Page

Abstract

Introduction

Conclusions

References

Tables

Figures

⏪

⏩

◀

▶

Back

Close

Full Screen / Esc

Printer-friendly Version

Interactive Discussion



emissions and boundary conditions. The derivatives with respect to model parameters are obtained by processing the adjoint variables Sandu et al. (2005a). The units of adjoint sensitivities with respect to a parameter are one over the units of that parameter (since the cost function (9) is unitless).

Figure 8 presents the adjoint sensitivities of the 4-D-Var cost function (9) with respect to several model parameters. The linearization is performed around the 4-D-Var solution (10), i.e., around a forward trajectory that starts with optimized initial ozone concentrations. Consequently, the sensitivity of the 4-D-Var cost function with respect to the initial ozone concentration is very small (in theory is equal to zero, as it represents the gradient value at a minimum point). However, the sensitivities with respect to the initial CO (Fig. 8a), NO_x (Fig. 8b), and PAN (Fig. 8c) concentrations are not small. Consequently, TES ozone profiles provide information that can potentially constrain ozone precursor initial conditions as well. More importantly, Fig. 8d displays the sensitivity of the 4-D-Var cost function with respect to total NO_x emissions. These sensitivities indicate that ozone observations can be used to constrain ozone precursor emissions as well. This point is explored in the context of a 4-D-Var chemical box model in Hamer et al. (2011). The strong sensitivity of the atmospheric chemical state to boundary conditions differentiates the chemical data assimilation problem from the traditional numerical weather prediction problem. Consequently, even in condition where the 3-D-Var solution may have similar performance to the 4-D-Var solution, the ability to assess the sensitivities of the innovations in the 3-D-Var to boundary and initial conditions through adjoint calculations provides important tools for a more detailed investigation of processes controlling that distribution.

6.3.2 Direct comparison of 3-D-Var and 4-D-Var corrections

Due to the different times when they incorporate observations, it is difficult to perform a direct comparison comparison of the ways 3-D-Var and 4-D-Var use this information. An assessment of the two analyses can be done at the end of the assimilation interval.

Comparison of chemical data assimilation schemes

K. Singh et al.

Title Page

Abstract

Introduction

Conclusions

References

Tables

Figures

⏪

⏩

◀

▶

Back

Close

Full Screen / Esc

Printer-friendly Version

Interactive Discussion



The comparison against ozonesonde data, presented in Figs. 2 and 5, uses analysis data at different times throughout the assimilation window.

We propose a variational approach to compare the net effect of all corrections performed by the 3-D-Var, with the 4-D-Var correction of the state. This comparison provides insight into how each method injects information from observations into the state (at a specific time). We discuss three approaches, based on “pulling back” to the initial time and adding all corrections performed by 3-D-Var, pulling back and adding all the differences between the 3-D-Var and the 4-D-Var analyses, and finding an equivalent initial condition for 3-D-Var.

To be specific, we first quantify the cumulative effect of all 3-D-Var corrections, in order to study how 3-D-Var builds the analysis. Since the 3-D-Var corrections take place at different times, they need to first be brought to the same time. For example, this can be done by “propagating backwards” the 3-D-Var correction at t_i to the initial time t_0 , through the adjoint \mathbf{M}_i^T of the tangent linear model $\mathbf{M}_i = \partial \mathbf{x}_i / \partial \mathbf{x}_0$. The cumulative effect of all 3-D-Var corrections at the initial time is

$$\sum_{i=0}^N \mathbf{M}_k^T \cdot \mathbf{P}_i^{f(3)} \mathbf{H}_i^T \left(\mathbf{H}_i \mathbf{P}_i^{f(3)} \mathbf{H}_i^T + \mathbf{R}_i \right)^{-1} \left(\mathbf{x}_i^{\text{obs}} - \mathcal{H}(\mathbf{x}_i^{f(3)}) \right). \quad (22)$$

Here $\mathbf{x}_i^{f(3)}$ and $\mathbf{P}_i^{f(3)}$ are the 3-D-Var forecast state and the forecast covariance at t_i , respectively.

This approach allows for the assessment of the cumulative effect of all 3-D-Var corrections at the initial time, and to directly compare the 3-D-Var and 4-D-Var via the corresponding changes in initial conditions.

Next, we seek to estimate the discrepancy between the analyses generated by the 3-D-Var and by the 4-D-Var methods. Let the free model run (background), the 4-D-Var, and the 3-D-Var analyses at t_i be \mathbf{x}_i^b , $\mathbf{x}_i^{a(4)}$, $\mathbf{x}_i^{a(3)}$, respectively. Define the following “discrepancy” cost function that measures the difference between the 4-D-Var and the 3-D-Var analyses at all times

Comparison of chemical data assimilation schemes

K. Singh et al.

Title Page

Abstract

Introduction

Conclusions

References

Tables

Figures

◀

▶

◀

▶

Back

Close

Full Screen / Esc

Printer-friendly Version

Interactive Discussion



$$\mathcal{D}(\mathbf{x}_0^{a(4)}) = \frac{1}{2} \sum_{i=0}^N \left\| \mathbf{x}_i^{a(4)} - \mathbf{x}_i^{a(3)} \right\|_{\mathbf{Q}_i^{-1}}^2. \quad (23)$$

The gradient of the discrepancy function with respect to the initial conditions is given by the adjoint model, using a linearization of the forward model about the 4-D-Var analysis trajectory

$$\nabla_{\mathbf{x}_0^a} \mathcal{D}(\mathbf{x}_0^{a(4)}) = \sum_{i=0}^N \mathbf{M}_i^T \mathbf{Q}_i^{-1} (\mathbf{x}_i^{a(4)} - \mathbf{x}_i^{a(3)}), \quad \text{where } \mathbf{M}_i = \frac{\partial \mathbf{x}_i^{a(4)}}{\partial \mathbf{x}_0^{a(4)}}. \quad (24)$$

Here \mathbf{M}_i is the linearized model solution operator about the 4-D-Var analysis trajectory. Each term in the discrepancy sum is weighed by the (covariance-like) matrix \mathbf{Q}_i , which is assumed to be invertible. This adjoint considers the differences between the 4-D-Var and the 3-D-Var analyses at different times, and pulls all these differences back to time t_0 . The cumulative discrepancy between the two analyses, as given by this metric, reads

$$\text{diff}(\mathbf{x}^{a(4)}, \mathbf{x}^{a(3)}) = \nabla_{\mathbf{x}_0^a} \mathcal{D}(\mathbf{x}_0^{a(4)}). \quad (25)$$

Finally, we want to determine the “3-D-Var equivalent initial condition” $\mathbf{x}_0^{e(3)}$, such that the resulting trajectory $\mathbf{x}_i^{e(3)}$, $i \geq 1$, fits best the 3-D-Var analysis at the final time $\mathbf{x}_N^{a(3)}$, in a least squares sense:

$$\mathbf{x}_0^{e(3)} = \underset{\mathbf{x}_0}{\text{argmin}} \beta(\mathbf{x}_0^{e(3)}) = \frac{1}{2} \left\| \mathbf{x}_N^{e(3)} - \mathbf{x}_N^{a(3)} \right\|_{\mathbf{Q}_N^{-1}}^2.$$

To our knowledge, no attempt has been made to date to estimate the equivalent effect of all 3-D-Var corrections at the initial time. (Note that the 3-D-Var analysis is not

Comparison of chemical data assimilation schemes

K. Singh et al.

Title Page

Abstract

Introduction

Conclusions

References

Tables

Figures

◀

▶

◀

▶

Back

Close

Full Screen / Esc

Printer-friendly Version

Interactive Discussion



a trajectory of the model). The methodology is explained in Appendix A. The least squares solution to finding the 3-D-Var equivalent initial condition is (A3)

$$\mathbf{x}_0^{e(3)} = \mathbf{x}_0^{a(4)} - \left(\mathbf{M}_N^T \mathbf{Q}_N^{-1} \mathbf{M}_N \right)^{-1} \cdot \mathbf{M}_N^T \mathbf{Q}_N^{-1} \left(\mathbf{x}_N^{e(3)} - \mathbf{x}_N^{a(3)} \right),$$

The 3-D-Var solution incorporates all the observation information when it reaches t_N , the end of the assimilation window. For a direct comparison with the 4-D-Var initial condition, the 3-D-Var equivalent initial condition match the 3-D-Var analysis only at the final time.

5 Similar to (23), a cost function that measures the discrepancy between the 3-D-Var and the free model forecast at all times can be defined. This gradient involves an adjoint run, with a linearization performed about the free model run (background) trajectory.

Figure 9 displays results for the metric (25), i.e., the sum of all analysis discrepancies between the 3-D-Var and the 4-D-Var ozone analyses, projected to time t_0 along with differences between the free running model and the initial conditions inferred from the 4-D-Variational solution. All scaling covariances are taken to be the identity matrix, $\mathbf{Q}_i = \mathbf{I}$, $i = 0, \dots, N$. Interestingly, significant corrections to the initial conditions in the 4-D-Var solution are made poleward of 60° N even though there is no TES data used that directly covers that region. These positive corrections can be explained by strong transport from higher latitudes into the mid-latitudes characterized by the transport adjoint sensitivities of the mid-latitude innovations with the TES data. Similar features are seen though in the opposite sign in Fig. 9d through the cumulative back projection in the 3-D-Var solution.

7 Conclusions

20 This paper compares the performance of 3-D-Var, 4-D-Var, and suboptimal Kalman filter data assimilation systems, applied to the estimation of global tropospheric ozone distribution. The data is provided by TES ozone profile retrievals. The study uses the

Comparison of chemical data assimilation schemes

K. Singh et al.

Title Page

Abstract

Introduction

Conclusions

References

Tables

Figures

⏪

⏩

◀

▶

Back

Close

Full Screen / Esc

Printer-friendly Version

Interactive Discussion



3-D-Var and 4-D-Var data assimilation frameworks we have implemented into GEOS-Chem v7. Two different assimilation window lengths (five days and two weeks) are considered. The quality of the ozone analyses provided by different assimilation schemes is verified against ozonesonde measurements, an independent data set.

5 The three approaches have different computational costs. The suboptimal Kalman filter is the least expensive, followed closely by 3-D-Var. 4-D-Var has the highest memory and computational costs as it requires checkpointing dependent variables, and performs both a forward and an adjoint model run for every iteration.

10 All three data assimilation systems are able to improve ozone estimates using TES profile retrievals. For the five days assimilation window the sequential methods, 3-D-Var and suboptimal KF, perform similarly: they decrease the relative difference between mean analysis and ozonesonde measurements to about 5–20 %. 4-D-Var, on the other hand, brings this error down to less than 4 %, for up to 180 hPa. For the two weeks assimilation window the performance of the sequential methods changes with different height levels. In the lower and mid troposphere 3-D-Var performs better, while in the mid to upper troposphere the suboptimal Kalman filter analysis is more accurate. The relative error (measured against ozonesonde data) is 4–16 % for the sequential analyses, and is less than 4 % for up to 150 hPa for 4-D-Var. The corrections of ozone concentration performed by the sequential assimilation methods are localized along the satellite orbit. On the other hand, the 4-D-Var solution is physically and chemically self-consistent over the assimilation window. The region between latitudes 30° N to 60° N has the greatest impact from all the assimilation systems. This region extends up to 90° N in case of 4-D-Var, which accounts for the transport of high latitude ozone into the mid-latitudes. However, we should caution that the IONS datasets were primarily over North America. Therefore, we can not assess whether the increased northern mid-latitude ozone concentrations lead to a more accurate analysis.

25 A method to directly compare the analyses provided different schemes is proposed, based on “pulling back” differences to the initial time, as discussed in Sect. 6.3.2. The calculations show that the 4-D-Var corrections are larger than those provided by

Comparison of chemical data assimilation schemes

K. Singh et al.

[Title Page](#)[Abstract](#)[Introduction](#)[Conclusions](#)[References](#)[Tables](#)[Figures](#)[⏪](#)[⏩](#)[◀](#)[▶](#)[Back](#)[Close](#)[Full Screen / Esc](#)[Printer-friendly Version](#)[Interactive Discussion](#)

Comparison of chemical data assimilation schemes

K. Singh et al.

Title Page

Abstract

Introduction

Conclusions

References

Tables

Figures

⏪

⏩

◀

▶

Back

Close

Full Screen / Esc

Printer-friendly Version

Interactive Discussion



3-D-Var. The adjoint sensitivity analysis in Sect. 6.3.1 reveals that 4-D-Var has the intrinsic capability of capturing mechanistic relationships between multiple chemical species, and between emissions and concentrations fields. In a similar vein, this adjoint analysis can be used in conjunction with other assimilation schemes (3-D-Var, suboptimal KF) to interrogate what model parameters are driving the residual differences with the observations.

The comparison results presented here will guide the choice of the best assimilation scheme for the problem at hand. The sub-optimal Kalman filter and the 3-D-Var solution provide useful solutions that do not require significant changes as the forward model physics and chemistry are updated. By virtue of their simplicity, they make less model assumptions, e.g., all differences between observation and forecast can be attributed to initial conditions, and therefore can be robust under a variety of conditions. On the other hand, the 4-D-Var approach provides a physically consistent solution where uncertainties are ascribed to a combination of initial and boundary conditions. This physical consistency makes it more straightforward to interpret and make scientific inferences. We have introduced a new method that applies the adjoint sensitivity to help interpret the 3-D-Var solutions, which provides a kind of middle ground between the more efficient 3-D-Var approach and the more sophisticated 4-D-Var approaches. Interesting extensions of the GEOS-Chem data assimilation framework, such as efficient information content estimation of observations and construction of full rank covariance matrices, are discussed in companion papers Singh et al. (2011a,b,c).

Appendix A

The 3-D-Var equivalent initial condition

Finally, we want to determine the “3-D-Var equivalent initial condition” $\mathbf{x}_0^{e(3)}$ such that the resulting trajectory fits best the 3-D-Var analysis in a least squares sense. To our knowledge, no attempt has been made to date to estimate the equivalent effect of all

3-D-Var corrections at the initial time. (Note that the 3-D-Var analysis is not a trajectory of the model). The dynamic equations for the 3-D-Var trajectory, linearized about the 4-D-Var analysis, read:

$$\mathbf{x}_i^{a(3)} - \mathbf{x}_i^{a(4)} = \mathbf{M}_i \cdot (\mathbf{x}_0^{e(3)} - \mathbf{x}_0^{a(4)}) + \theta_i, \quad i = 0, \dots, N. \quad (\text{A1})$$

The errors $\theta_i = \mathbf{x}_i^{a(3)} - \mathbf{x}_i^{a(4)}$ are assumed to be normally distributed with mean zero and covariance \mathbf{Q}_i . We now seek the equivalent 3-D-Var initial condition that solves (A1) in a least squares sense. The scaled linearized dynamic equations are

$$\mathbf{Q}_i^{-1/2} \mathbf{M}_i (\mathbf{x}_0^{e(3)} - \mathbf{x}_0^{a(4)}) - \mathbf{Q}_i^{-1/2} (\mathbf{x}_i^{a(3)} - \mathbf{x}_i^{a(4)}) = \mathbf{Q}_i^{-1/2} \theta_i, \quad i = 0, \dots, N,$$

and involve the scaled residuals $\mathbf{Q}_i^{-1/2} \theta_i$ which are standard normal random vectors. Therefore the least squares solution is the one that minimizes the sum of scaled residual norms squared

$$\mathbf{x}_0^{e(3)} = \operatorname{argmin} \sum_{i=0}^N \left\| \mathbf{M}_i (\mathbf{x}_0^{e(3)} - \mathbf{x}_0^{a(4)}) - (\mathbf{x}_i^{a(3)} - \mathbf{x}_i^{a(4)}) \right\|_{\mathbf{Q}_i^{-1}}^2.$$

The minimum of this quadratic function is obtained by imposing that its gradient equals zero. This leads to the following system of linear equations:

$$\underbrace{\left(\sum_{i=0}^N \mathbf{M}_i^T \mathbf{Q}_i^{-1} \mathbf{M}_i \right)}_{\nabla_{\mathbf{x}_0^a, \mathbf{x}_0^a}^2 \mathcal{D}(\mathbf{x}_0^{a(4)})} (\mathbf{x}_0^{e(3)} - \mathbf{x}_0^{a(4)}) = \underbrace{\sum_{i=0}^N \mathbf{M}_i^T \mathbf{Q}_i^{-1} (\mathbf{x}_i^{a(3)} - \mathbf{x}_i^{a(4)})}_{\nabla_{\mathbf{x}_0^a} \mathcal{D}(\mathbf{x}_0^{a(4)})}.$$

Therefore the least squares solution to finding the 3-D-Var equivalent initial condition is

$$\mathbf{x}_0^{e(3)} = \mathbf{x}_0^{a(4)} - \left(\nabla_{\mathbf{x}_0^a, \mathbf{x}_0^a}^2 \mathcal{D}(\mathbf{x}_0^{a(4)}) \right)^{-1} \cdot \nabla_{\mathbf{x}_0^a} \mathcal{D}(\mathbf{x}_0^{a(4)}). \quad (\text{A2})$$

Consider a standard normal random perturbation is applied at t_0 to the 4-D-Var optimal initial condition. This perturbation is propagated through the linearized model, and its covariance at t_i is $\mathbf{M}_i \mathbf{M}_i^T$. Let $\mathbf{Q}_i = \rho_i \mathbf{M}_i \mathbf{M}_i^T$ in (23) in order to account for an increasing error with the model evolution. The scalar weights ρ_i decrease with i , to account for the reduction in uncertainty through 3-D-Var assimilation, and are chosen such that $\sum_{i=0}^N \rho_i = 1$. Using the fact that $\mathbf{M}_i^T \mathbf{Q}_i^{-1} \mathbf{M}_i = \mathbb{I}$ for all i we have that the equivalent 3-D-Var initial solution is

$$\mathbf{x}_0^{e(3)} = \mathbf{x}_0^{a(4)} - \sum_{k=0}^N \mathbf{M}_k^T \mathbf{Q}_k^{-1} (\mathbf{x}_0^{a(4)} - \mathbf{x}_0^{a(3)}) = \mathbf{x}_0^{a(4)} - \nabla_{\mathbf{x}_0^a} \mathcal{D}(\mathbf{x}_0^{a(4)}).$$

The 3-D-Var solution has incorporated all the observation information when it reaches t_N , the end of the assimilation window. Therefore it makes sense to choose $\rho_0 = \dots = \rho_{N-1} = 0$ and $\rho_N = 1$ in order to have the equivalent initial condition match the 3-D-Var analysis only at the final time. In this case

$$\mathbf{x}_0^{e(3)} = \mathbf{x}_0^{a(4)} - \left(\mathbf{M}_N^T \mathbf{Q}_N^{-1} \mathbf{M}_N \right)^{-1} \mathbf{M}_N^T \mathbf{Q}_N^{-1} (\mathbf{x}_0^{a(4)} - \mathbf{x}_0^{a(3)}). \quad (\text{A3})$$

Acknowledgements. This work was supported by NASA through the ROSES-2005 AIST project. The work of A. Sandu was also partially supported by NSF through the award NSF DMS-0915047.

The authors would like to thank Anne Thompson of Pennsylvania State University and David Tarasick of Environment Canada who led the IONS-6 campaign, and who provided the IONS data used in this work.

**Comparison of
chemical data
assimilation schemes**

K. Singh et al.

Title Page

Abstract

Introduction

Conclusions

References

Tables

Figures

◀

▶

◀

▶

Back

Close

Full Screen / Esc

Printer-friendly Version

Interactive Discussion



References

- Beer, R., Glavich, T. A., and Rider, D. M.: Tropospheric emission spectrometer for the Earth Observing System's Aura satellite, *Appl. Optics*, 40(15), 2356–2367, 2001. 5, 12
- Bei, N., de Foy, B., Lei, W., Zavala, M., and Molina, L. T.: Using 3DVAR data assimilation system to improve ozone simulations in the Mexico City basin, *Atmos. Chem. Phys.*, 8, 7353–7366, doi:10.5194/acp-8-7353-2008, 2008. 4
- Benkovitz, C. M., Scholtz, M. T., Pacyna, J., Tarrason, L., Dignon, J., Voldner, E. C., Spiro, P. A., Logan, J. A., and Graedel, T. E.: Global gridded inventories of anthropogenic emissions of sulfur and nitrogen, *J. Geophys. Res.*, 101(D22), 29239–29253, 1996. 11
- Bey, I., Jacob, D. J., Yantosca, R. M., Logan, J. A., Field, B., Fiore, A. M., Li, Q., Liu, H., Mickley, L. J., and Schultz, M.: Global modeling of tropospheric chemistry with assimilated meteorology: Model description and evaluation, *J. Geophys. Res.*, 106, 23073–23096, 2001. 11
- Blum, J., Le Dimet, F. X., and Navon, I. M.: Data Assimilation for Geophysical Fluids, Chapter in *Computational Methods for the Atmosphere and the Oceans*, Volume 14, Elsevier Science Ltd, New York, ISBN-13: 978-0-444-51893-4, 2009.
- Boutahar, J., Lacour, S., Mallet, V., Quélo, D., Roustan, Y., and Sportisse, B.: Development and validation of a fully modular platform for numerical modelling of air pollution: POLAIR, *Int. J. Environ. Pollut.*, 22(1/2), 17–28, 2004.
- Bowman, K. W., Worden, J., Steck, T., Worden, H. M., Clough, S., and Rodgers, C.: Capturing time and vertical variability of tropospheric ozone: A study using TES nadir retrievals, *J. Geophys. Res.*, 107(D23), 4723, doi:10.1029/2002JD002150, 2002. 13
- Bowman, K. W., Rodgers, C. D., Kulawik, S. S., Worden, J., Sarkissian, E., Osterman, G., Steck, T., Ming Lou, Eldering, A., Shephard, M., Worden, H., Lampel, M., Clough, S., Brown, P., Rinsland, C., Gunson, M., and Beer, R.: Tropospheric Emission Spectrometer: Retrieval method and error analysis, *IEEE T. Geosci. Remote*, 44(5), 1297–1307, 2006. 12, 13
- Bowman, K. W., Jones, D. B. A., Logan, J. A., Worden, H., Boersma, F., Chang, R., Kulawik, S., Osterman, G., Hamer, P., and Worden, J.: The zonal structure of tropical O₃ and CO as observed by the Tropospheric Emission Spectrometer in November 2004 - Part 2: Impact of surface emissions on O₃ and its precursors, *Atmos. Chem. Phys.*, 9, 3563–3582, doi:10.5194/acp-9-3563-2009, 2009.
- Carmichael, G. R., Sandu, A., Chai, T., Daescu, D., Constantinescu, E. M., and Tang, Y.:

Comparison of chemical data assimilation schemes

K. Singh et al.

Title Page

Abstract

Introduction

Conclusions

References

Tables

Figures

◀

▶

◀

▶

Back

Close

Full Screen / Esc

Printer-friendly Version

Interactive Discussion



Comparison of chemical data assimilation schemes

K. Singh et al.

Title Page

Abstract

Introduction

Conclusions

References

Tables

Figures

◀

▶

◀

▶

Back

Close

Full Screen / Esc

Printer-friendly Version

Interactive Discussion



Predicting air quality: Improvements through advanced methods to integrate models and measurements, *J. Comput. Phys.*, 227(7), 3540–3571, 2008. 4

Chai, T., Carmichael, G. R., Sandu, A., Tang, Y., and Daescu, D. N.: Chemical data assimilation of transport and chemical evolution over the Pacific (TRACE-P) aircraft measurements, *J. Geophys. Res.*, 111, D02301, doi:10.1029/2005JD005883, 2006.

Chai, T., Carmichael, G. R., Tang, Y., Sandu, A., Hardesty, M., Pilewskie, P., Whitlow, S., Browell, E. V., Avery, M. A., Thouret, V., Nedelec, P., Merrill, J. T., and Thomson, A. M.: Four dimensional data assimilation experiments with ICARTT (International Consortium for Atmospheric Transport and Transformation) ozone measurements, *J. Geophys. Res.*, 112, D12S15, doi:10.1029/2006JD007763, 2007. 4

Chai, T., Carmichael, G. R., Tang, Y., and Sandu, A.: Regional NO_x emission inversion through a four-dimensional variational approach using SCIAMACHY tropospheric NO₂ column observations, *Atmos. Environ.*, 43, 5046–5055, doi:10.1016/j.atmosenv.2009.06.052, 2009. 4

Clark, H. L., Cathala, M.-L., Teyssèdre, H., Cammas, J.-P., and Peuch, V.-H.: Cross-tropopause fluxes of ozone using assimilation of MOZAIC observations in a global CTM, *Tellus B*, 59, 39–49, 2006. 5, 6

Cohn, S., Da Silva, A., Guo, J., Sienkiewicz, M., and Lamich, D.: Assessing the Effects of Data Selection with DAO's Physical-space Statistical Analysis System, *Mon. Weather Rev.*, 126, 2913–2926, 1998. 4

Constantinescu, E. M., Sandu, A., Chai, T., and Carmichael, G. R.: Investigation of ensemble-based chemical data assimilation in an idealized setting, *Atmos. Environ.*, 41(1), 18–36, 2007a. 5

Constantinescu, E. M., Sandu, A., Chai, T., and Carmichael, G. R.: Ensemble-based chemical data assimilation. I: General approach, *Quarterly J. Roy. Meteor. Soc.*, 133(626), 1229–1243, 2007b. 5, 6

Constantinescu, E. M., Sandu, A., Chai, T., and Carmichael, G. R.: Ensemble-based chemical data assimilation. II: Covariance localization, *Q. J. Roy. Meteor. Soc.*, 133(626), 1245–1256, 2007c. 5, 6, 20

Cooper, O. R., Stohl, A., Trainer, M., Thompson, A. M., Witte, J. C., Oltmans, S. J., Morris, G., Pickering, K. E., Crawford, J. H., Chen, G., Cohen, R. C., Bertram, T. H., Wooldridge, P., Perring, A., Brune, W. H., Merrill, J., Moody, J. L., Tarasick, D., Nedelec, P., Forbes, G., Newchurch, M. J., Schmidlin, F. J., Johnson, B. J., Turquety, S., Baughcum, S. L., Ren, X., Fehsenfeld, F. C., Meagher, J. F., Spichtinger, N., Brown, C. C., McKeen, S. A., McDermid, I.

Comparison of chemical data assimilation schemes

K. Singh et al.

Title Page

Abstract

Introduction

Conclusions

References

Tables

Figures

◀

▶

◀

▶

Back

Close

Full Screen / Esc

Printer-friendly Version

Interactive Discussion



S., and Leblanc, T.: Large upper tropospheric ozone enhancements above midlatitude North America during summer: In situ evidence from the IONS and MOZAIC ozone measurement network, *J. Geophys. Res.*, 111, D24S05, doi:10.1029/2006JD007306, 2006.

Cooper, O. R., Trainer, M., Thompson, A. M., Oltmans, S. J., Tarasick, D. W., Witte, J. C., Stohl, A., Eckhardt, S., Lelieveld, J., Newchurch, M. J., Johnson, B. J., Portmann, R. W., Kalnajs, L., Dubey, M. K., Leblanc, T., McDermid, I. S., Forbes, G., Wolfe, D. E., Carey-Smith, T., Morris, G. A., Lefer, B., Rappenglück, B., Joseph, E., Schmidlin, F., Meagher, J. F., Fehsenfeld, F. C., Keating, T. J., Van Curen, R. A., and Minschwaner, K.: Evidence for a recurring eastern North American upper tropospheric ozone maximum during summer, *J. Geophys. Res.*, 112, D23304, doi:10.1029/2007JD008710, 2007.

Courtier, P. and Talagrand, O.: Variational assimilation of meteorological observations with the adjoint vorticity equations II: Numerical results, *Q. J. Roy. Meteor. Soc.*, 113, 1329–1347, 1987. 6

Courtier, P., Andersson, E., Heckley, W., Pailleux, J., Vasiljevic, D., Hamrud, M., Hollingsworth, A., Rabier, F., and Fisher, M.: The ECMWF implementation of three-dimensional variational assimilation (3-D-Var) I: Formulation, *Q. J. Roy. Meteor. Soc.*, 124(550), 1783–1807, 1998. 4

Daescu, D. N.: On the sensitivity equations of four-dimensional variational (4-D-Var) data assimilation, *Mon. Weather Rev.*, 136(8), 3050–3065, 2008.

Daescu, D., Carmichael, G. R., and Sandu, A.: Adjoint Implementation of Rosenbrock Methods Applied to Variational Data Assimilation Problems, *J. Comp. Phys*, 165, 496–510, 2000. 18
Daescu, D., Sandu, A., and Carmichael, G.R.: Direct and Adjoint Sensitivity Analysis of Chemical Kinetic Systems with KPP: II – Validation and Numerical Experiments, *Atmos. Environ.*, 37, 5097–5114, 2003. 18

Daley, R.: *Atmospheric Data Analysis*, Cambridge University Press, p. 457 pp., 1991. 4

Damian, V., Sandu, A., Damian, M., Potra, F., and Carmichael, G.R.: The Kinetic PreProcessor KPP – A Software Environment for Solving Chemical Kinetics, *Comp. and Chem. Eng.*, 26, 11, 1567–1579, 2002. 18

Derber, J. C., Parrish, D. F., and Lord, S. J.: The New Global Operational Analysis System at the National Meteorological Center, *Weather Forecast.*, 6, 538–547, 1991. 4

Duncan, B. N., Martin, R. V., Staudt, A. C., Yevich, R., and Logan, J. A.: Interannual and seasonal variability of biomass burning emissions constrained by satellite observations, *J. Geophys. Res.*, 108(D2), 4100, doi:10.1029/2002JD002378, 2003. 11

- Elbern, H. and Schmidt, H.: Ozone episode analysis by four dimensional variational chemistry data assimilation, *J. Geophys. Res.*, 106(D4), 3569–3590, 2001. 4
- Eller, P., Singh, K., Sandu, A., Bowman, K., Henze, D. K., and Lee, M.: Implementation and evaluation of an array of chemical solvers in the Global Chemical Transport Model GEOS-Chem, *Geosci. Model Dev.*, 2, 89–96, doi:10.5194/gmd-2-89-2009, 2009. 12, 19
- 5 Evensen, G.: Sequential data assimilation with a nonlinear quasi-geostrophic model using Monte Carlo methods to forecast error statistics, *J. Geophys. Res.*, 99, 10143–10162, 1994. 5
- Geer, A. J., Lahoz, W. A., Bekki, S., Bormann, N., Errera, Q., Eskes, H. J., Fonteyn, D., Jackson, D. R., Juckes, M. N., Massart, S., Peuch, V.-H., Rharmili, S., and Segers, A.: The ASSET intercomparison of ozone analyses: method and first results, *Atmos. Chem. Phys.*, 6, 5445–5474, doi:10.5194/acp-6-5445-2006, 2006. 5, 6
- 10 Gaspari, G. and Cohn, S. E.: Construction of correlation functions in two and three dimensions, *Q. J. Roy. Meteor. Soc.*, Vol 125 Issue 554,7 23–757, 1999.
- 15 Gauthier, P., Charette, C., Fillion, L., Koclas, P., and Laroche, S.: Implementation of a 3-D Variational Data Assimilation System at the Canadian Meteorological Centre. Part I: The Global Analysis, *Atmos. Ocean*, 37(2), 103-156, 1999. 4
- Hakami, A., Henze, D. K., Seinfeld, J. H., Chai, T., Tang, Y., Carmichael, G. R., and Sandu, A.: Adjoint inverse modeling of black carbon during ACE-Asia, *J. Geophys. Res.*, 110, D14301, doi:10.1029/2004JD005671, 2005. 4
- 20 Hakami, A., Henze, D. K., Seinfeld, J. H., Singh, K., Sandu, A., Kim, S., Byun, D., and Li, Q.: The adjoint of CMAQ, *Environ. Sci. Technol.*, 41(22), 7807–7817, 2007. 4
- Hamer, P. D., Bowman, K. W., and Henze, D. K.: Observing requirements for geostationary satellites to enable ozone air quality prediction, *Atmos. Chem. Phys. Discuss.*, 11, 19291–19355, doi:10.5194/acpd-11-19291-2011, 2011. 26
- 25 Henze, D. K., Seinfeld, J. H., Liao, W., Sandu, A., and Carmichael, G. R.: Inverse modeling of aerosol dynamics: Condensational growth. *J. Geophys. Res.-Atmos.*, 109(D14), D14201, doi:10.1029/2004JD004593, 2004. 4
- Henze, D. K., Hakami, A., and Seinfeld, J. H.: Development of the adjoint of GEOS-Chem, *Atmos. Chem. Phys.*, 7, 2413–2433, doi:10.5194/acp-7-2413-2007, 2007. 4, 12, 19
- 30 Henze, D. K., Seinfeld, J. H., and Shindell, D. T.: Inverse modeling and mapping US air quality influences of inorganic PM_{2.5} precursor emissions using the adjoint of GEOS-Chem, *Atmos. Chem. Phys.*, 9, 5877–5903, doi:10.5194/acp-9-5877-2009, 2009. 5, 12

**Comparison of
chemical data
assimilation schemes**K. Singh et al.

[Title Page](#)[Abstract](#)[Introduction](#)[Conclusions](#)[References](#)[Tables](#)[Figures](#)[⏪](#)[⏩](#)[◀](#)[▶](#)[Back](#)[Close](#)[Full Screen / Esc](#)[Printer-friendly Version](#)[Interactive Discussion](#)

**Comparison of
chemical data
assimilation schemes**

K. Singh et al.

[Title Page](#)[Abstract](#)[Introduction](#)[Conclusions](#)[References](#)[Tables](#)[Figures](#)[◀](#)[▶](#)[◀](#)[▶](#)[Back](#)[Close](#)[Full Screen / Esc](#)[Printer-friendly Version](#)[Interactive Discussion](#)

Horowitz, L. W.: Past, present and future concentrations of tropospheric ozone and aerosols: Methodology, ozone evaluation, and sensitivity to aerosol wet removal, *J. Geophys. Res.*, 111, D22211, doi:10.1029/2005JD006937, 2006.

Horowitz, L. W., Walters, S., Mauzerall, D. L., Emmons, L. K., Rasch, P. J., Granier, C., Tie, X., Lamarque, J., Schultz, M. G., Tyndall, G. S., Orlando, J. J., and Brasseur, G. P.: A global simulation of tropospheric ozone and related tracers: Description and evaluation of MOZART, version 2, *J. Geophys. Res.*, 108(D24), 4784, doi:10.1029/2002JD002853, 2003.

Houtekamer, P. L., Mitchell, H. L., Pellerin, G., Buehner, M., Charron, M., Spacek, L., and Hansen, B.: Atmospheric Data Assimilation with an Ensemble Kalman Filter: Results with Real Observations, *Mon. Weather Rev.*, 133(3), 604–620, 2005. 5

Hudman, R. C., Jacob, D. J., Turquety, S., Leibensperger, E. M., Murray, L. T., Wu, S., Gilliland, A. B., Avery, M., Bertram, T. H., Brune, W., Cohen, R. C., Dibb, J. E., Flocke, F. M., and Fried, A.: Surface and lightning sources of nitrogen oxides over the United States: Magnitudes, chemical evolution and outflow, *J. Geophys. Res.*, 112, D12S05, doi:10.1029/2006JD007912, 2007.

Jacob, D. J.: *Introduction to Atmospheric Chemistry*, Princeton University Press, New Jersey, 1999. 3

Jones, D. B. A., Bowman, K. W., Palmer, P. I., Worden, J. R., Jacob, D. J., Hoffman, R. N., Bey, I. and Yantosca, R. M.: Potential of observations from the Tropospheric Emission Spectrometer to constrain continental sources of carbon monoxide, *J. Geophys. Res.*, 108(D24), 4789, doi:10.1029/2003JD003702, 2003. 13

Jones, D. B. A., Bowman, K. W., Logan, J. A., Heald, C. L., Liu, J., Luo, M., Worden, J., and Drummond, J.: Inversion analysis of carbon monoxide emissions using data from the TES and MOPITT satellite instruments, *Atmos. Chem. Phys. Discuss.*, 7, 17625–17662, doi:10.5194/acpd-7-17625-2007, 2007.

Kalnay, E.: *Atmospheric modeling, data assimilation and predictability*, Cambridge University Press, 2002. 4

Khattatov, B. V., Gille, J. C., Lyjak, L. V., Brasseur, G. P., Dvortsov, V. L., Roche, A. E., and Walters, J.: Assimilation of photochemically active species and a case analysis of UARS data, *J. Geophys. Res.*, 104, 18715–18737, 1999.

Khattatov, B. V., Lamarque, J.-F., Lyjak, L. V., Menard, R., Levelt, P., Tie, X., Brasseur, G. P., and Gille, J. C.: Assimilation of satellite observations of long-lived chemical species in global chemistry transport models, *J. Geophys. Res.*, 105(D23), 29–135, 2000. 4, 5, 6, 10, 19

Comparison of chemical data assimilation schemes

K. Singh et al.

Title Page

Abstract

Introduction

Conclusions

References

Tables

Figures

◀

▶

◀

▶

Back

Close

Full Screen / Esc

Printer-friendly Version

Interactive Discussion



- Kopacz, M., Jacob, D. J., Henze, D. K., Heald, C. L., Streets, D. G. and Zhang, Q.: A comparison of analytical and adjoint Bayesian inversion methods for constraining Asian sources of CO using satellite (MOPITT) measurements of CO columns, *J. Geophys. Res.*, 114, D04305, doi:10.1029/2007JD009264, 2007. 12
- 5 Lahoz, W. A., Geer, A. J., Bekki, S., Bormann, N., Ceccherini, S., Elbern, H., Errera, Q., Eskes, H. J., Fonteyn, D., Jackson, D. R., Khatatov, B., Marchand, M., Massart, S., Peuch, V.-H., Rharmili, S., Ridolfi, M., Segers, A., Talagrand, O., Thornton, H. E., Vik, A. F., and von Clarmann, T.: The Assimilation of Envisat data (ASSET) project, *Atmos. Chem. Phys.*, 7, 1773–1796, doi:10.5194/acp-7-1773-2007, 2007.
- 10 Lamarque, J.-F., Khatatov, B. V., and Gille, J. C.: Constraining tropospheric ozone column through data assimilation, *J. Geophys. Res.*, 107(D22), 4651, doi:10.1029/2001JD001249, 2002. 5, 6
- Laroche, S., Dorval, E. C., Canada, Q. C., Gauthier, P., Tanguay, M., Pellerin, S., and Morneau, J.: Evaluation of the operational 4-D-Var at the Meteorological Service of Canada, 21st
15 Conference on Weather Analysis and Forecasting, 14B.3, 2005. 5
- LeDimet, F.-X. and Talagrand, O.: Variational algorithms for analysis and assimilation of meteorological observations: theoretical aspects, *Tellus A*, 38, 97–110, 1986. 6
- Li, Z. and Navon, I. M.: Optimality of variational data assimilation and its relationship with the Kalman filter and smoother, *Q. J. R. Meteorol. Soc.*, 127, 661–683, 2001. 5
- 20 Li, Q., Jacob, D. J., Park, R. J., Wang, Y., Heald, C. L., Hudman, R. C., Yantosca, R. M., Martin, R. V., and Evans, M. J.: North American pollution outflow and the trapping of convectively lifted pollution by upper-level anticyclone, *J. Geophys. Res.*, 110, D10301, doi:10.1029/2004JD005039, 2005.
- Liao, W. Y., Sandu, A., Carmichael, G. R., and Chai, T.: Singular vector analysis for atmospheric chemical transport models, *Mon. Weather Rev.*, 134(9), 2443–2465, 2006. 5
- 25 Lions, J. L.: *Optimal control of systems governed by partial differential equations*, Springer-Verlag, 1971. 6
- Logan, J. A.: Trends in the vertical distribution of ozone: An analysis of ozonesonde data, *J. Geophys. Res.*, 99(D12), 25553–25585, 1994. 3
- 30 Logan, J. A.: An analysis of ozonesonde data for the troposphere: Recommendations for testing 3-D models and development of a gridded climatology for tropospheric ozone, *J. Geophys. Res.*, 104(D13), 16115–16149, 1999. 3
- McLinden, C. A., Olsen, S. C., Hannegan, B., Wild, O., Prather, M. J., and Sundet, J.: Strato-

Comparison of chemical data assimilation schemes

K. Singh et al.

Title Page

Abstract

Introduction

Conclusions

References

Tables

Figures

◀

▶

◀

▶

Back

Close

Full Screen / Esc

Printer-friendly Version

Interactive Discussion



spheric ozone in 3-D models: A simple chemistry and the cross-tropopause flux, *J. Geophys. Res.*, 105(D11), 14653-14665, doi:10.1029/2000JD900124, 2000. 15

Menard, R., Cohn, S. E., Chang, L.-P., and Lyster, P. M.: Assimilation of stratospheric chemical tracer observations using a Kalman Filter I: Formulation, *Mon. Weather Rev.*, 128, 2654–2671, 2000. 5, 6, 11

Munro, R., Siddans, R., Reburn, W. J., and Kerridge, B. J.: Direct measurement of tropospheric ozone distributions from space, *Nature*, 392(6672), 168-171, 1998. 3

Nassar, R., Logan, J. A., Worden, H. M., Megretskaia, I. A., Bowman, K. W., Osterman, G. B., Thompson, A. M., Tarasick, D. W., Austin, S., Claude, H., Dubey, M. K., Hocking, W. K., Johnson, B. J., Joseph, E., Merrill, J., Morris, G. A., Newchurch, M., Oltmans, S. J., Posny, F.ç., Schmidlin, F. J., Vömel, H., Whiteman, D. N., and Witte, J. C.: Validation of Tropospheric Emission Spectrometer (TES) nadir ozone profiles using ozonesonde measurements, *J. Geophys. Res.*, 113, D15S17, doi:10.1029/2007JD008819, 2008. 14, 21

Navon, I. M.: Data assimilation for Numerical Weather Prediction: a review, in: *Data Assimilation for Atmospheric, Oceanic, and Hydrologic Applications*, XVIII, 475 p. 326 illus., Hardcover, ISBN: 978-3-540-71055-4, 2009. 4

Oltmans, S. J., Lefohn, A. S., Harris, J. M., Galbally, I., Scheel, H. E., Bodeker, G., Brunke, E., Claude, H., Tarasick, D., Johnson, B. J., Simmonds, P., Shadwick, D., Anlauf, K., Hayden, K., Schmidlin, F., Fujimoto, T., Akagi, K., Meyer, C., Nichol, S., Davies, J., Redondas, A., and Cuevas, E.: Long-term changes in tropospheric ozone, *Atmos. Environ.*, 40, 3156-3173, 2006. 3

Ott, E., Hunt, B. R., Szunyogh, I., Zimin, A. V., Kostelich, E. J., Kostelich, M., Corazza, M., Sauer, T., Kalnay, E., Patil, D. J., and Yorke, J. A.: A local ensemble Kalman Filter for Atmospheric Data Assimilation, *Tellus A*, 56, 415–428, 2004.

Palmer, P. I., Jacob, D. J., Jones, D. B. A., Heald, C. L., Yantosca, R. M., Logan, J. A., and Sachse, G. W. and Streets, D. G.: Observations over the western Pacific, *J. Geophys. Res.*, 108(D21), 8828, doi:10.1029/2003JD003397, 2003.

Parrington, M., Jones, D. B. A., Bowman, K. W., Horowitz, L. W., Thompson, A. M., Tarasick, D. W., and Witte, J. C.: Estimating the summertime tropospheric ozone distribution over North America through assimilation of observations from the Tropospheric Emission Spectrometer, *J. Geophys. Res.*, 113, D18307, doi:10.1029/2007JD009341, 2008. 20

Parrington, M., Jones, D. B. A., Bowman, K. W., Thompson, A. M., Tarasick, D. W., Merrill, J., Oltmans, S. J., Leblanc, T., Witte, J. C., and Millet, D. B.: Impact of the assimilation of

- ozone from the tropospheric emission spectrometer on surface ozone across North America, *Geophys. Res. Lett.*, 36(4), L04802, doi:10.1029/2008GL036935, 2009. 5, 6, 11, 13, 14
- Parrish, D. F. and Derber, J. C.: The national meteorological center's spectral statistical-interpolation analysis system, *Mon. Weather Rev.*, 120, 1747–1763, 1992. 4
- 5 Pierce, R. B., Schaack, T., Al-Saadi, J. A., Fairlie, T. D., Kittaka, C., Lingenfelter, G., Natarajan, M., Olson, J., Soja, A., Zapotocny, T., Lenzen, A., Stobie, J., Johnson, D., Avery, M. A., Sachse, G. W., Thompson, A., Cohen, R., Dibb, J. E., Crawford, J., Rault, D., Martin, R., Szykman, J., and Fishman, J.: Chemical data assimilation estimates of continental U. S. ozone and nitrogen budgets during the Intercontinental Chemical Transport Experiment-North America, *J. Geophys. Res.*, 112, D12S21, doi:10.1029/2006JD007722, 2007. 5, 6
- 10 Pierce, R. B., Al-Saadi, J., Kittaka, C., Schaack, T., Lenzen, A., Bowman, K., Szykman, J., Soja, A., Ryerson, T., Thompson, A. M., Bhartia, P., and Morris, G. A.: Impacts of background ozone production on Houston and Dallas, Texas, air quality during the Second Texas Air Quality Study field mission. *J. Geophys. Res.*, 114, D00F09, , doi:10.1029/2008JD011337, 2009. 5
- 15 Pires, C., Vautard, R., and Talagrand, O.: On extending the limits of variational assimilation in nonlinear chaotic systems, *Tellus A*, 48, 96–121, 1996.
- Price, C. and Rind, D.: A Simple Lightning Parameterization for Calculating Global Lightning Distributions, *J. Geophys. Res.*, 97(D9), 9919–9933, doi:10.1029/92JD00719, 1992. 11
- 20 Rabier, F., Jarvinen, H., Klinker, E., Mahfouf, J.-F., and Simmons, A.: The ECMWF operational implementation of four-dimensional variational data assimilation I: Experimental results with simplified physics, *Q. J. Roy. Meteor. Soc.*, 126, 1143–1170, 2000. 4
- Sandu, A. and Zhang, L.: Discrete second order adjoints in atmospheric chemical transport modeling, *J. Comput. Phys.*, 227(12), 5949–5983, 2008.
- 25 Sandu, A., Daescu, D., and Carmichael, G. R.: Direct and Adjoint Sensitivity Analysis of Chemical Kinetic Systems with KPP: I – Theory and Software Tools, *Atmos. Environ.*, 37(36), 5083–5096, 2003a. 18
- Sandu, A., Daescu, D., and Carmichael, G. R.: Direct and adjoint sensitivity analysis of chemical kinetic systems with KPP: II – Numerical validation and applications, *Atmos. Environ.*, 37(36), 5097–5114, 2003b. 18
- 30 Sandu, A., Daescu, D. N., Carmichael, G. R., and Chai, T.: Adjoint sensitivity analysis of regional air quality models, *J. Comput. Phys.*, 204, 222–252, 2005a. 4, 15, 26
- Sandu, A., Liao, W., Carmichael, G. R., Henze, D. K., and Seinfeld, J. H.: Inverse modeling

Comparison of chemical data assimilation schemes

K. Singh et al.

[Title Page](#)[Abstract](#)[Introduction](#)[Conclusions](#)[References](#)[Tables](#)[Figures](#)[◀](#)[▶](#)[◀](#)[▶](#)[Back](#)[Close](#)[Full Screen / Esc](#)[Printer-friendly Version](#)[Interactive Discussion](#)

- of aerosol dynamics using adjoints: Theoretical and numerical considerations, *Aerosol Sci. Technol.*, 39(8), 677–694, 2005b. 4
- Sasaki, Y. K.: An objective analysis based on the variational method, *J. Met. Soc. Jap.* II(36), 77–88, 1958. 6
- 5 Segers, A. J., Eskes, H. J., Van Der A, R. J., Van Oss, R. F., and Van Velthoven, P. F. J.: Assimilation of GOME ozone profiles and a global chemistry-transport model, using a Kalman Filter with anisotropic covariance, *Q. J. Roy. Meteor. Soc.*, 131, 477–502, 2005. 5, 6
- Singh, K., Eller, P., Sandu, A., Bowman, K. W., Jones, D. B. A., and Lee, M.: Improving GEOS-Chem model forecasts through profile retrievals from Tropospheric Emission Spectrometer, in: *Lecture Notes on Computational Science*, 5545, 302–311, International Conference on Computational Science 2009, Baton Rouge, Louisiana, May 25–27, 2009a. 12
- 10 Singh, K., Eller, P., Sandu, A., Henze, D., Bowman, K. W., Kopacz, M., and Lee, M.: Towards the construction of a standard adjoint GEOS-Chem model, High Performance Computing Symposium (HPC 2009) at Spring Simulation Multiconference (SpringSim'09), San Diego, California, March 22–27, 2009b. 12, 14
- 15 Singh, K., Jardak, M., Sandu, A., Bowman, K., Lee, M., and Jones, D.: Construction of non-diagonal background error covariance matrices for global chemical data assimilation, *Geosci. Model Dev.*, 4, 299–316, doi:10.5194/gmd-4-299-2011, 2011a. 18, 19, 31
- Singh, K., Sandu, A., Jardak, M., Bowman, K. W., and Lee, M.: A Practical Method to Estimate Information Content in the Context of 4-D-VAR Data Assimilation, *J. Geophys. Res.*, submitted, 2011b. 21, 31
- 20 Singh, K. and Sandu, A.: Variational Chemical Data Assimilation with Approximate Adjoint, *Computers & Geosciences-Elsevier*, submitted, doi:10.1016/j.cageo.2011.07.003, 2011c. 24, 31
- 25 Stevenson, D. S., Dentener, F. J., Schultz, M. G., Ellingsen, K., Van Noije, T. P. C., Wild, O., Zeng, G., Amann, M., Atherton, C. S., Bell, N., Bergmann, D. J., Bey, I., Butler, T., Cofala, J., Collins, W. J., Derwent, R. G., Doherty, R. M., Drevet, J., Eskes, H. J., Fiore, A. M., Gauss, M., Hauglustaine, D. A., Horowitz, L. W., Isaksen, I. S. A., Krol, M. C., Lamarque, J.-F., Lawrence, M. G., Montanaro, V., Müller, J.-F., Pitari, G., Prather, M. J., Pyle, J. A., Rast, S., Rodriguez, J. M., Sanderson, M. G., Savage, N. H., Shindell, D. T., Strahan, S. E., Sudo, K., and Szopa, S.: Multimodel ensemble simulations of present-day and near-future tropospheric ozone, *J. Geophys. Res.*, 111, D08301, doi:10.1029/2005JD006338, 2006.
- 30 Tang, Y. H., Carmichael, G. R., Horowitz, L. W., Uno, I., Woo, J. H., Streets, D. G., Dabdub, D.,

Comparison of chemical data assimilation schemes

K. Singh et al.

Title Page

Abstract

Introduction

Conclusions

References

Tables

Figures

◀

▶

◀

▶

Back

Close

Full Screen / Esc

Printer-friendly Version

Interactive Discussion



Comparison of chemical data assimilation schemes

K. Singh et al.

[Title Page](#)
[Abstract](#)
[Introduction](#)
[Conclusions](#)
[References](#)
[Tables](#)
[Figures](#)
[◀](#)
[▶](#)
[◀](#)
[▶](#)
[Back](#)
[Close](#)
[Full Screen / Esc](#)
[Printer-friendly Version](#)
[Interactive Discussion](#)


Kurata, G., Sandu, A., Allan, J., Atlas, E., Flocke, F., Huey, L. G., Jakoubek, R. O., Millet, D. B., Quinn, P. K., Roberts, J. M., Worsnop, D. R., Goldstein, A., Donnelly, S., Schauffler, S., Stroud, V., Johnson, K., Avery, M. A., Singh, H. B., and Apel, E. C.: Multiscale simulations of tropospheric chemistry in the Eastern Pacific and on the US West Coast during spring 2002, *J. Geophys. Res.-Atmos.*, 109(D23), D23S11, doi:10.1029/2004JD004513, 2004. 4

Tarasick, D. W., Fioletov, V. E., Wardle, D. I., Kerr, J. B., and Davies, J.: Changes in the vertical distribution of ozone over Canada from ozonesondes: 1980-2001, *J. Geophys. Res.*, 110, D02304, doi:10.1029/2004JD004643, 2005. 3

Tellmann, S., Rozanov, V. V., Weber, M., and Burrows, J. P.: Improvements in the tropical ozone profile retrieval from GOME-UV/Vis nadir spectra, *Adv. Space Res.*, 34(4), 739-743, 2004. 3

TES Science Team, TES L2 Data Users Guide, Jet Propulsion Laboratory, California Institute of Technology, Pasadena, California, available at: <http://tes.jpl.nasa.gov/uploadedfiles/TESDataUsersGuideV4.0.pdf>, 2006.

Thompson, A. M., Stone, J. B., Witte, J. C., Miller, S. K., Pierce, R. B., Chatfield, R. B., Oltmans, S. J., Cooper, O. R., Loucks, A. L., Taubman, B. F., Johnson, B. J., Joseph, E., Kucsera, T. L., Merrill, J. T., Morris, G. A., Hersey, S., Forbes, G., Newchurch, M. J., Schmidlin, F. J., Tarasick, D. W., Thouret V., and Cammas, J. P.: Intercontinental chemical transport experiment ozonesonde network study (IONS) 2004: 1. Summertime upper troposphere/lower stratosphere ozone over northeastern North America, *J. Geophys. Res.*, 112 D12S12, doi:10.1029/2006JD007441, 2007a. 19

Thompson, A. M., Stone, J. B., Witte, J. C., Miller, S. K., Oltmans, S. J., Kucsera, T. L., Ross, K. L., Pickering, K. E., Merrill, J. T., Forbes, G., Tarasick, D. W., Joseph, E., Schmidlin, F. J., McMillan, W. W., Warner, J., Hints, E. J., and Johnson, J. E.: Intercontinental chemical transport experiment ozonesonde network study (IONS) 2004: 2. Tropospheric ozone budgets and variability over northeastern North America, *J. Geophys. Res.*, 112 D12S13, doi:10.1029/2004JD005359, 2007b.

Todling, R. and Cohn, S. E.: Suboptimal Schemes for Atmospheric Data Assimilation Based on the Kalman Filter, *Mon. Weather Rev.*, 122, 2530–2557, 1994.

Worden, J. R., Bowman, K. W., and Jones, D. B. A.: Characterization of atmospheric profile retrievals from Limb Sounding Observations of an inhomogeneous atmosphere, *J. Quant. Spectrosc. Radiat. Trans.*, 86, 45–71, 2004. 13

Wu, L., Mallet, V., Bocquet, M., and Sportisse, B.: A comparison study of data assimilation algorithms for ozone forecasts, *J. Geophys. Res.*, 113, D20310, doi:10.1029/2008JD009991,

2008. 5, 20, 24

Yevich, R. and Logan, J. A.: An assessment of biofuel use and burning of agricultural waste in the developing world, *Global Biogeochem. Cy.*, 17(4), 1095, doi:10.1029/2002GB001952, 2003. 12

5 Zhang, L., Constantinescu, E. M., Sandu, A., Tang, Y., Chai, T., Carmichael, G. R., Byun, D., and Olaguer, E.: An adjoint sensitivity analysis and 4-D-Var data assimilation study of Texas air quality, *Atmos. Environ.*, 42(23), 5787–5804, 2008. 4

Zhang, L., Jacob, D. J., Kopacz, M., Henze, D. K., Singh, K., and Jaffe, D. A.: Intercontinental source attribution of ozone pollution at western U.S. sites using an adjoint method, *Geophys. Res. Lett.*, 36, L11810, doi:10.1029/2009GL037950, 2009. 12

10 Zhu, C., Byrd, R. H., and Nocedal, J.: L-BFGS-B: Algorithm 778: L-BFGS-B, FORTRAN routines for large scale bound constrained optimization, *ACM Transactions on Mathematical Software*, 23(4), 550–560, 1997.

15

ACPD

11, 1–54, 2011

Comparison of chemical data assimilation schemes

K. Singh et al.

Title Page

Abstract

Introduction

Conclusions

References

Tables

Figures

⏪

⏩

◀

▶

Back

Close

Full Screen / Esc

Printer-friendly Version

Interactive Discussion



Comparison of chemical data assimilation schemes

K. Singh et al.

Title Page

Abstract

Introduction

Conclusions

References

Tables

Figures

⏪

⏩

◀

▶

Back

Close

Full Screen / Esc

Printer-friendly Version

Interactive Discussion



Table 1. Timing results for GEOS-Chem free model runs using SMVGEAR and KPP chemistry, suboptimal Kalman filter, 3-D-Var and 4-D-Var data assimilations with diagonal background error covariance matrix for a 24 h simulation starting 00:00 GMT 1 August 2006.

Experiment Description	CPU Time
Free model run, SMVGEAR chemistry solver	2 min 50 s
Free model run, KPP chemistry solver	3 min 18 s
Suboptimal Kalman filter with diagonal \mathbf{P}^f	3 min 08 s
3-D-Var with diagonal \mathbf{B}	3 min 57 s
4-D-Var with diagonal \mathbf{B} (per model run)	16 min 51 s

Comparison of chemical data assimilation schemes

K. Singh et al.

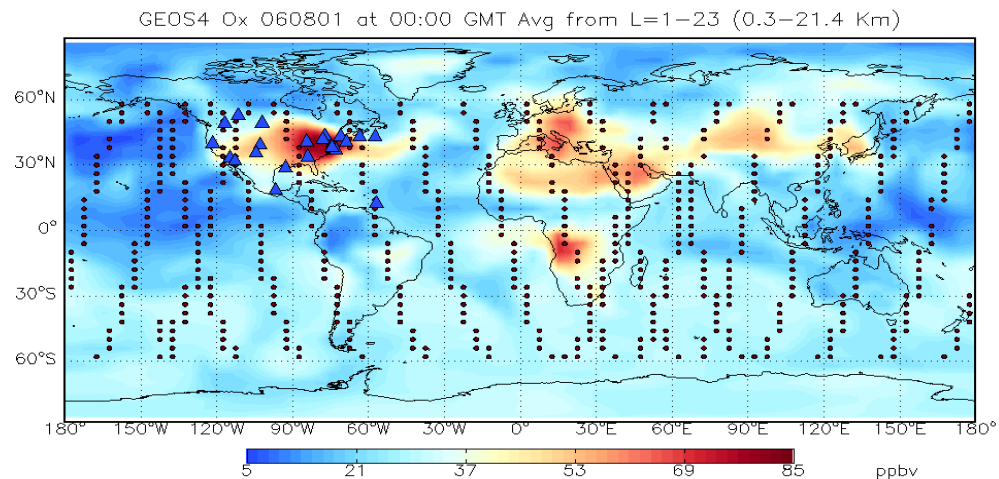


Fig. 1. Ozonesonde sounding stations (triangles) used during IONS06 campaign and AURA/TES satellite trajectory snapshots (dots) plotted over the global ozone distribution on 1 August 2006.

Title Page

Abstract

Introduction

Conclusions

References

Tables

Figures

◀

▶

◀

▶

Back

Close

Full Screen / Esc

Printer-friendly Version

Interactive Discussion



**Comparison of
chemical data
assimilation schemes**

K. Singh et al.

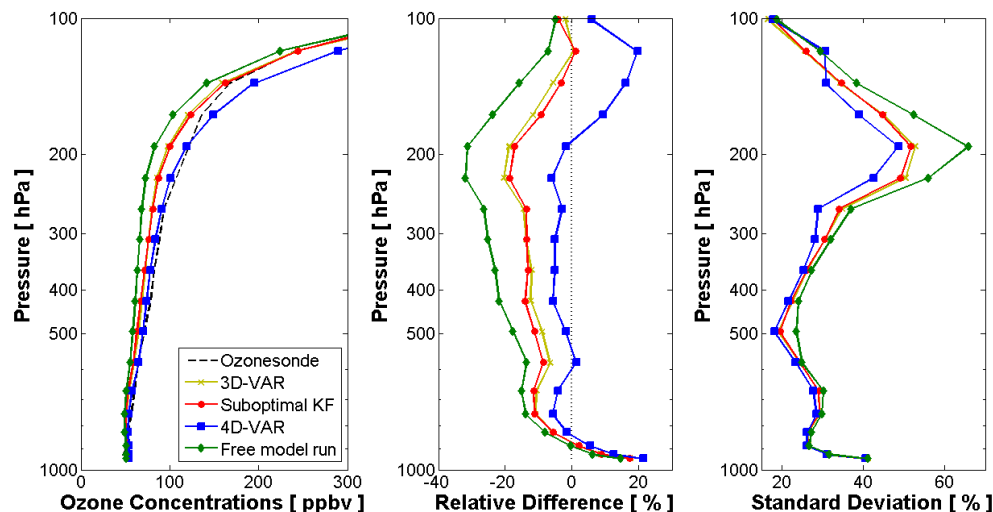


Fig. 2. The impact of ozone profile retrievals from TES on data assimilation systems for GEOS-Chem. Left panel: mean ozone concentrations sampled at ozonesonde locations and times for 3-D-Var, 4-D-Var, suboptimal KF analyses and free model trajectories. Center panel: relative mean errors of predicted ozone concentrations with respect to ozonesonde measurements. Right panel: standard deviation of absolute values of errors with respect to ozonesonde measurements. The data is averaged over all ozonesonde launches. These plots were generated from 5 days simulation from 00:00 GMT 1 August 2006 to 00:00 GMT 6 August 2006 and compared against ozonesonde data available for the month of August.

Title Page

Abstract

Introduction

Conclusions

References

Tables

Figures

◀

▶

◀

▶

Back

Close

Full Screen / Esc

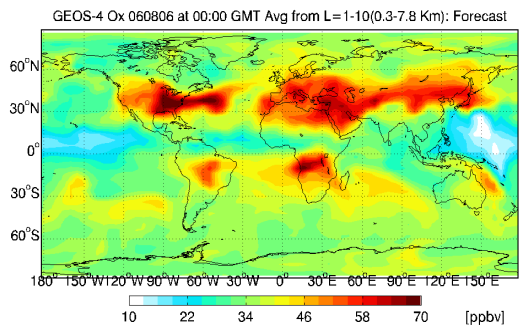
Printer-friendly Version

Interactive Discussion

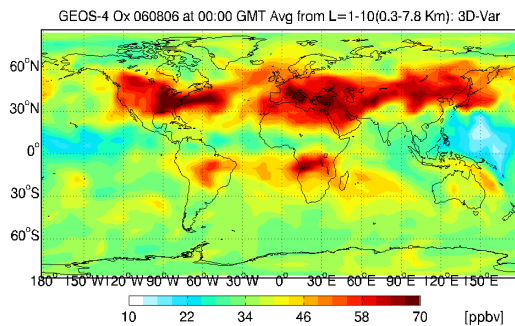


Comparison of chemical data assimilation schemes

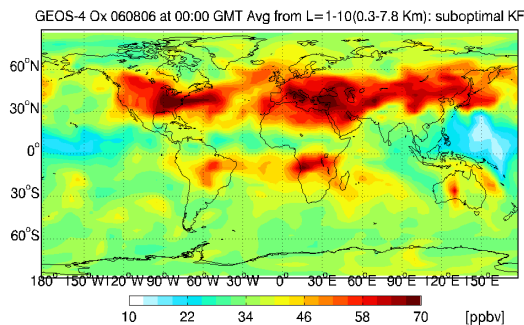
K. Singh et al.



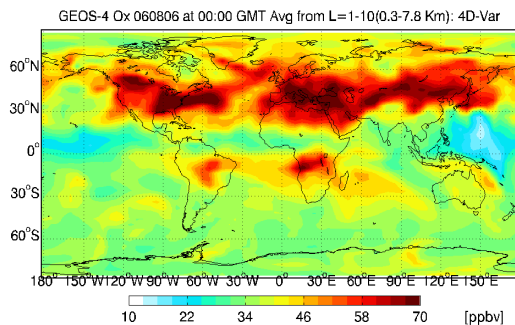
(a) Ozone forecast through free model run



(b) Ozone estimates through 3D-Var assimilation



(c) Ozone estimates through suboptimal Kalman filter



(d) Ozone estimates through 4D-Var assimilation

Fig. 3. Global ozone distribution at 00:00 GMT on 6 August 2006 averaged over the first 10 GEOS-Chem vertical levels. Panels (a–d): Global tropospheric ozone estimates provided by free model run and suboptimal KF, 3-D-Var, and 4-D-Var data assimilation systems from a 5-day simulation.

Title Page

Abstract

Introduction

Conclusions

References

Tables

Figures

◀

▶

◀

▶

Back

Close

Full Screen / Esc

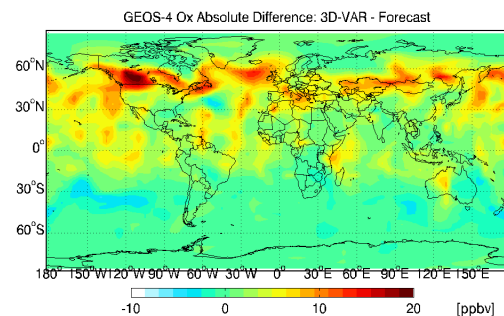
Printer-friendly Version

Interactive Discussion

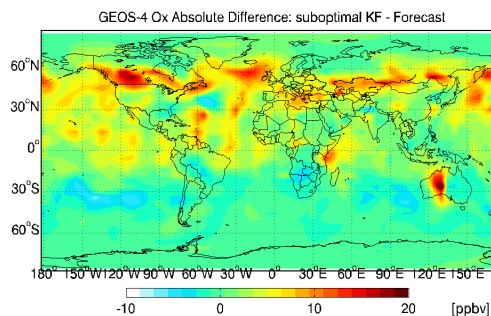


Comparison of chemical data assimilation schemes

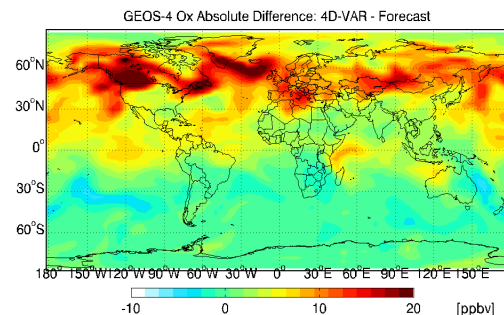
K. Singh et al.



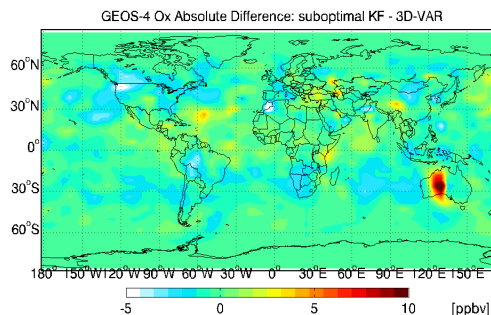
(a) Absolute difference between 3D-Var analysis and the free model run



(b) Absolute difference between suboptimal Kalman filter analysis and the free model run



(c) Absolute difference between 4D-Var analysis and the free model run



(d) Absolute difference between suboptimal Kalman filter and the 3D-Var analyses

Fig. 4. Differences in global ozone concentrations at 00:00 GMT on 6 August 2006, the end of 5-day simulation, averaged over first 10 GEOS-Chem vertical levels. Panels (a–c): Differences between suboptimal KF, 3-D-Var, and 4-D-Var analysis fields and the model forecast (solution without data assimilation). Panel (d): Difference between suboptimal KF and 3-D-Var analysis fields.

Title Page

Abstract

Introduction

Conclusions

References

Tables

Figures

◀

▶

◀

▶

Back

Close

Full Screen / Esc

Printer-friendly Version

Interactive Discussion



Comparison of chemical data assimilation schemes

K. Singh et al.

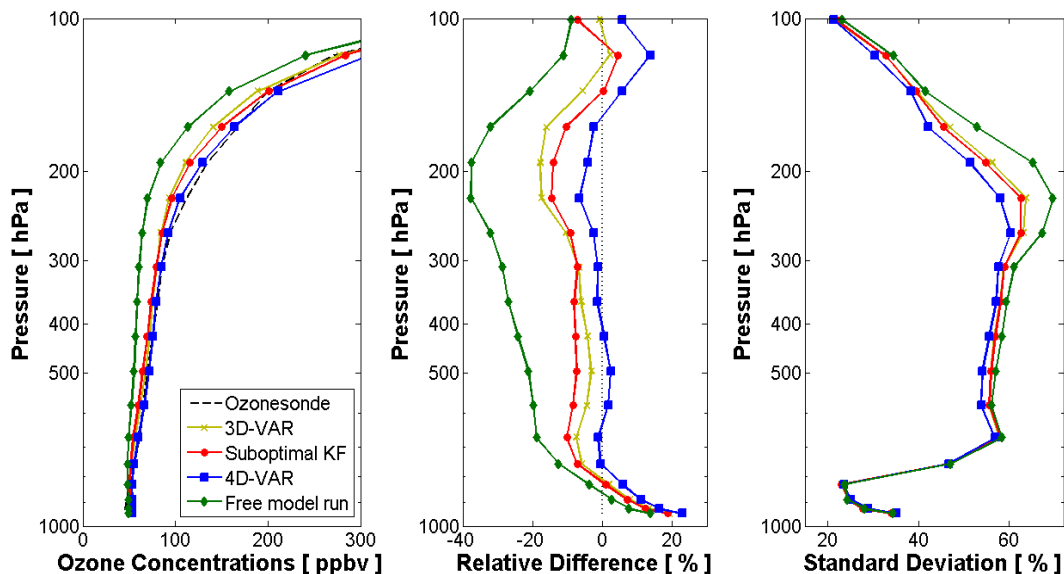


Fig. 5. The impact of ozone profile retrievals from TES on data assimilation systems for GEOS-Chem. Left panel: mean ozone concentrations at ozonesonde locations for 3-D-Var, 4-D-Var, suboptimal KF analyses and free model trajectories. Center panel: relative mean errors of predicted ozone concentrations with respect to ozonesonde measurements. Right panel: standard deviation of absolute values of errors with respect to ozonesonde measurements. The data is averaged over all ozonesonde launches. These plots were generated from 2 weeks simulation from 00:00 GMT 1 August 2006 to 00:00 GMT 15 August 2006 and compared against ozonesonde data available for the month of August.

Title Page

Abstract

Introduction

Conclusions

References

Tables

Figures

◀

▶

◀

▶

Back

Close

Full Screen / Esc

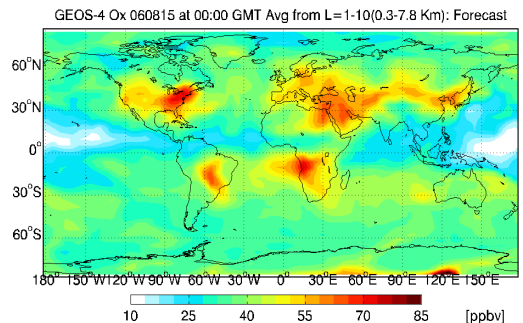
Printer-friendly Version

Interactive Discussion

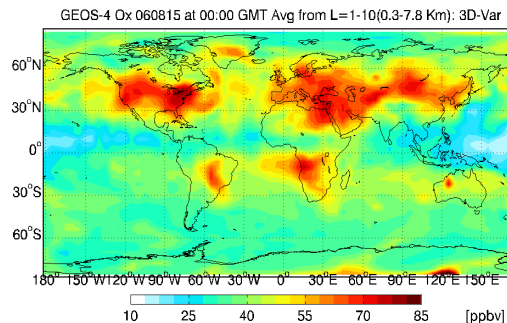


Comparison of chemical data assimilation schemes

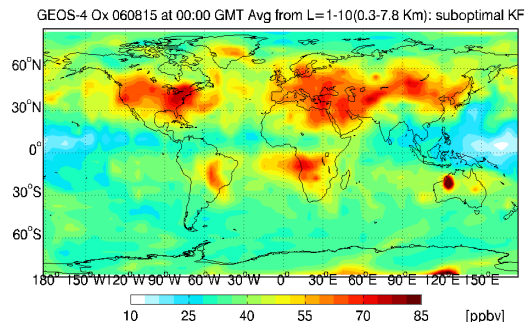
K. Singh et al.



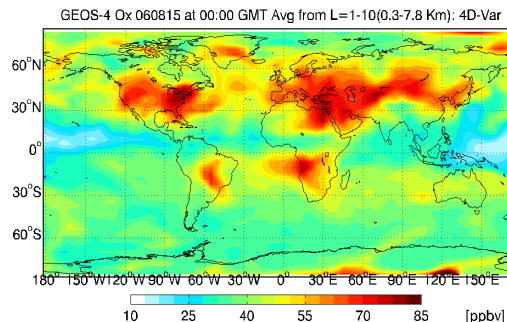
(a) Ozone forecast through free model run



(b) Ozone estimates through 3D-Var assimilation



(c) Ozone estimates through suboptimal Kalman filter



(d) Ozone estimates through 4D-Var assimilation

Fig. 6. Global ozone distribution at 00:00 GMT on 15 August 2006 averaged over the first 10 GEOS-Chem vertical levels. Panels (a–d): Global tropospheric ozone estimates provided by free model run and suboptimal KF, 3-D-Var, and 4-D-Var data assimilation systems from a 2-week simulation.

Title Page

Abstract

Introduction

Conclusions

References

Tables

Figures

◀

▶

◀

▶

Back

Close

Full Screen / Esc

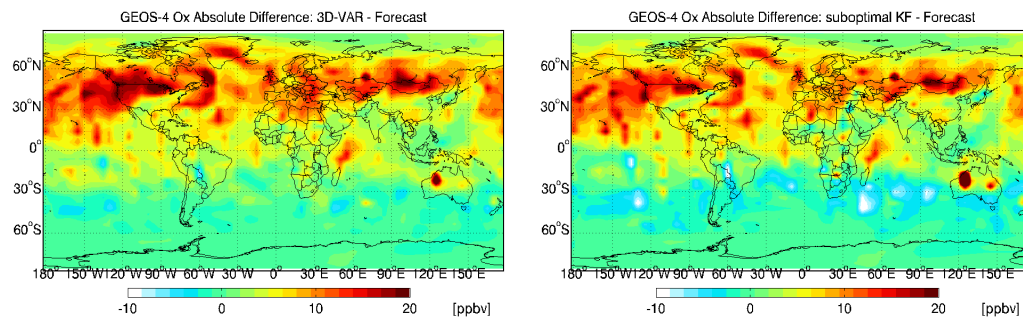
Printer-friendly Version

Interactive Discussion

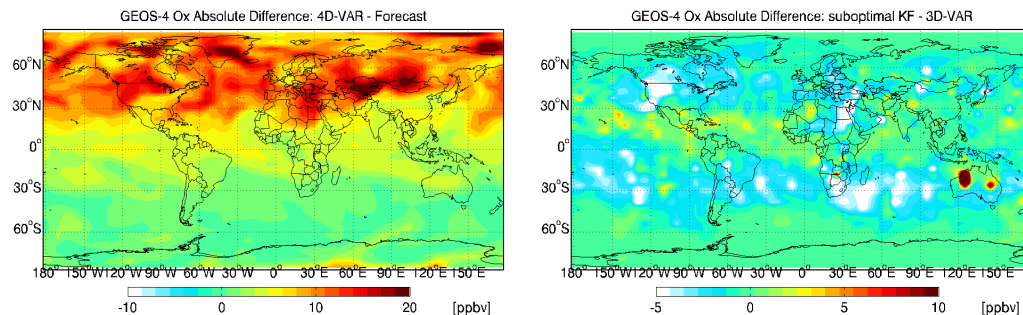


Comparison of chemical data assimilation schemes

K. Singh et al.



(a) Absolute difference between 3D-Var analysis and the free model run (b) Absolute difference between suboptimal Kalman filter analysis and the free model run



(c) Absolute difference between 4D-Var analysis and the free model run (d) Absolute difference between suboptimal Kalman filter and the 3D-Var analyses

Fig. 7. Differences in global ozone concentrations at 00:00 GMT on 15 August 2006, the end of 2-week simulation, averaged over first 10 GEOS-Chem vertical levels. Panels (a–c): Differences between suboptimal KF, 3-D-Var, and 4-D-Var analysis fields and the model forecast (solution without data assimilation). Panel (d): Difference between suboptimal KF and 3-D-Var analysis fields.

Title Page

Abstract

Introduction

Conclusions

References

Tables

Figures

◀

▶

◀

▶

Back

Close

Full Screen / Esc

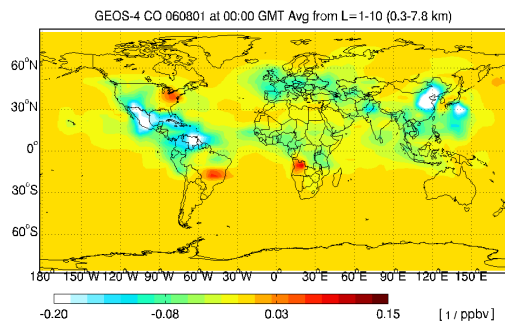
Printer-friendly Version

Interactive Discussion

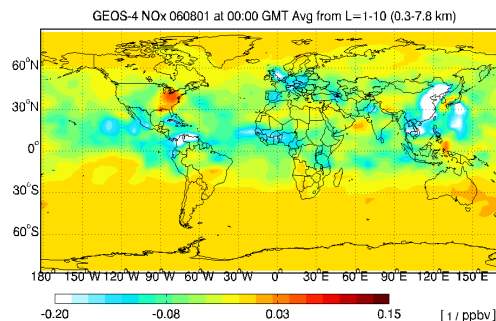


Comparison of chemical data assimilation schemes

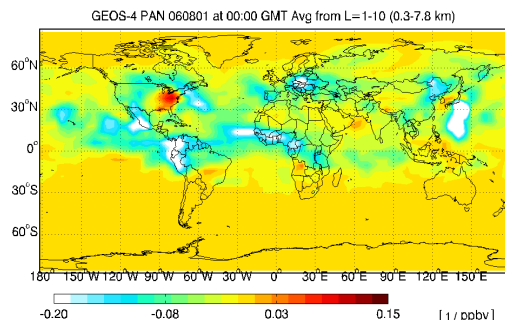
K. Singh et al.



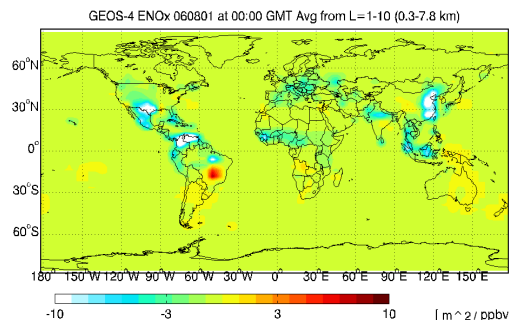
(a) Adjoint sensitivity with respect to CO initial conditions



(b) Adjoint sensitivity with respect to NO_x initial conditions



(c) Adjoint sensitivity with respect to PAN initial conditions



(d) Adjoint sensitivity with respect to NO_x emissions

Fig. 8. Adjoint sensitivities of the 4-D-Var cost function (9) with respect to different model parameters. The calculations correspond to the optimal initial ozone concentration. The 4-D-Var cost function involves differences between simulated and observed O_x. Panels (a), (b), (c) show sensitivities with respect to initial conditions of other chemical species (at 00:00 GMT on 1 August 2006). The sensitivities with respect to NO_x emissions in panel (d) correspond to emissions over the entire two-week assimilation window. All sensitivity fields are averaged over the first 10 GEOS-Chem vertical levels.

Title Page

Abstract

Introduction

Conclusions

References

Tables

Figures

◀

▶

◀

▶

Back

Close

Full Screen / Esc

Printer-friendly Version

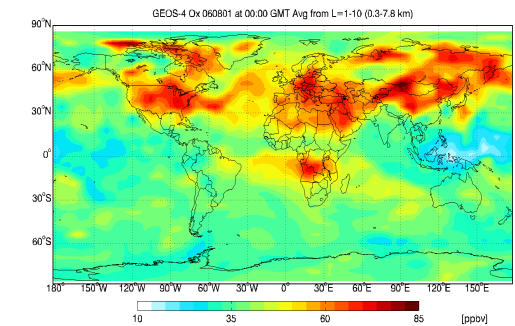
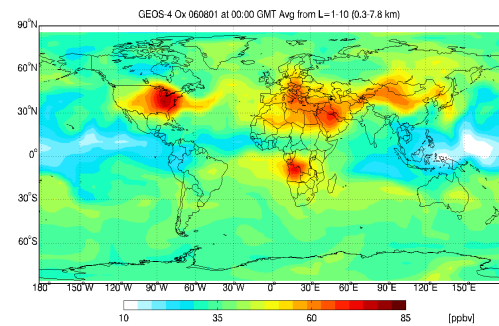
Interactive Discussion



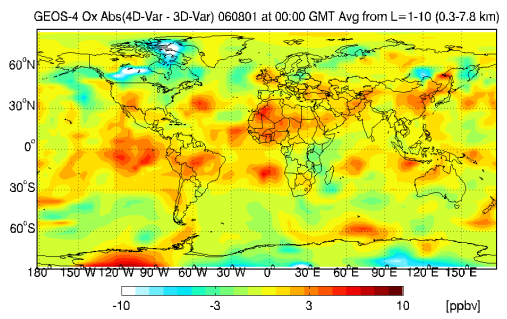
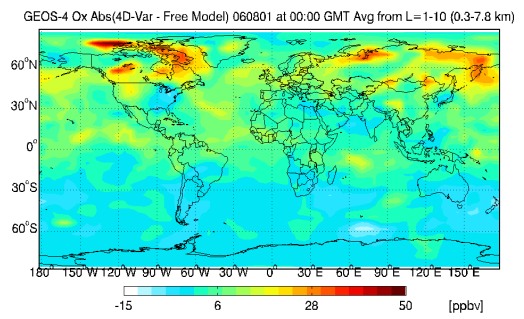
Comparison of chemical data assimilation schemes

K. Singh et al.

Title Page	
Abstract	Introduction
Conclusions	References
Tables	Figures
◀	▶
◀	▶
Back	Close
Full Screen / Esc	
Printer-friendly Version	
Interactive Discussion	



(a) Free model ozone concentration at the beginning of the assimilation window (b) 4D-Var ozone analysis at the beginning of the assimilation window



(c) Absolute difference between the 4D-Var optimal initial condition, and the background initial condition (d) Cumulative difference between the 4D-Var and 3D-Var analyses throughout the assimilation window

Fig. 9. The cumulative difference (25) between the 4-D-Var and the 3-D-Var ozone analyses, projected at the beginning of the five days assimilation window, and averaged over the first 10 GEOS-Chem vertical levels. A two-week long data assimilation window is used, starting at 00:00 GMT on 1 August 2006.

